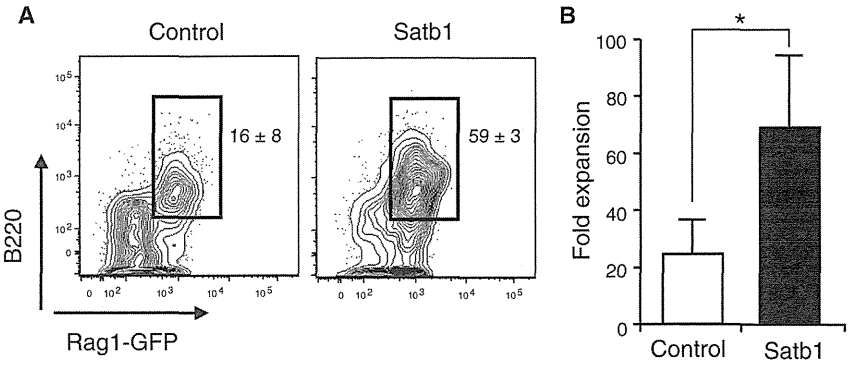

Figure 7. Satb1 Overexpression Restores Lymphopoietic Activity of Aged HSC

(A) Rag1/GFP$^-$ LSK cells were sorted from 2-year-old mice and retrovirally transduced with control or Satb1-DsRed vectors. Successfully transfected cells were cultured on OP9 cells. Cultures were established in triplicate. Numbers in each panel indicate the frequency of Rag1/GFP$^+$ CD45R/B220$^+$ cells.

(B) Yields of CD45R/B220$^+$ Rag1/GFP$^+$ Mac1$^-$ B-lineage cells per 1 input control- or Satb1-transduced Rag1/GFP-LSK cells were calculated and given as averages with SD bars. Statistical significance is *p < 0.05 (Figure 7; see also Figure S4).

lymphoid lineages even at the earliest stages. In addition, *Satb1*$^{-/-}$ HSCs are hindered in producing lymphocytes in vitro and in vivo that are consistent with the phenotypes originally described in *Satb1*$^{-/-}$ mice, suggesting an indispensable role of Satb1 in physiological lymphopoiesis.

Although we have previously identified molecules regulating early lymphoid differentiation, information about ones that initiate the process has been elusive (Oritani et al., 2000; Yokota et al., 2003b, 2008). The present study demonstrates that ectopic expression of Satb1 strongly induces differentiation toward lymphoid lineages and promotes lymphocyte growth from primitive progenitors, even when they are derived from aged BM or ESCs. We believe that these findings are important because they reveal that the earliest step of lymphopoiesis is affected by a global chromatin organizer. In addition, our results suggest that Satb1 expression could be a useful biomarker of aging and be manipulated to reverse immunosenescence.

Lymphoid-fate decisions are not necessarily determined by a few transcription factors or cytokines that positively regulate the differentiation in a hierarchical manner. The process should involve "closed windows" and "open opportunities." Gene array studies comparing HSC and ELP have shown that various lymphoid-related genes appear to be synchronously upregulated in ELP, whereas stem cell-related or myeloid-related ones are downregulated. From these observations, we speculated that a master regulator is present and involved in the synchronicity along with the hierarchical factors; further, we focused on the function of SATB1 in this process. Our results show that once Satb1 is substantially expressed in HSCs, it regulates hundreds of genes, including *Rag1*, *Il7*, *kitl*, and *Csf3r*, which together determine the lymphoid lineage fate. Satb1 itself has the determinant role in regulating a set of genes to exhibit the phenotype that we observed in vitro and in vivo experiments.

Increasing Satb1 beyond physiologic levels in HSCs and ESCs strongly augmented B lymphopoiesis, while depleting Satb1 from HSC dominantly impaired T lymphopoiesis in vivo. Satb1 overexpression in HSCs by itself induces an expression profile that favors B cell production. Conversely, Satb1 deficiency might have disrupted the delicate balance of Satb1 and other BUR-binding proteins such as Satb2 or Bright. We detected minimum levels of *Satb2* and *Bright* expression in WT HSC, and their expression levels significantly increase with B-lineage differentiation (data not shown). Interestingly, both genes were aberrantly induced in Satb1-deficient HSC (Table S2). Satb2 has a binding specificity similar to that of Satb1, and its expression is more predominant in the B lineage than in the T lineage (Dobreva et al., 2003). In ESCs, Satb2 function is antagonistic to Satb1 in regulating some target genes (Savarese et al., 2009). Whether these BUR-binding proteins are antagonistic or sometimes function synergistically, depending on cell differentiation or lineage remains unknown. Further studies of their functional correlation could yield important information about gene regulation in T and B lymphopoiesis.

Although our data provide evidence of a lymphocyte-inductive role of Satb1, an important question remains; that is, what regulates Satb1 expression? Depletion of long-lived mature B cells rejuvenates B-lymphopoiesis in old mice, suggesting that age-associated accumulation of aged B cells seems to be sensed by HSCs or early progenitors in BM (Keren et al., 2011). It will be interesting to learn whether such environmental cues influence Satb1 expression in HSCs. New strategies for boosting lymphocyte regeneration or protecting this capability during aging might emerge from studies of Satb1-related molecular mechanisms.

EXPERIMENTAL PROCEDURES

Animals

Animal studies were performed with the approval of the Institutional Review Board of Osaka University. Rag1-GFP knockin mice were previously described (Kuwata et al., 1999). *Satb1*$^{-/-}$ mice were also previously established (Alvarez et al., 2000). WT C57BL/6 mice and the congenic C57BL/6SJL strain (CD45.1 alloantigen) were obtained from Japan Clea (Shizuoka, Japan) and The Jackson Labs (Bar Harbor, ME), respectively. To obtain mouse fetuses, we considered the morning of the day of vaginal plug observation as E0.5.

Flow Cytometry and Cell Sorting

Cells were stained with Abs indicated in each experiment and analyzed with FACScanto or FACSaria (BD Bioscience). Adult BM cells from Rag1-GFP heterozygotes were used to isolate Lin$^-$ c-kit^{hi} Sca-1$^+$ Flt3$^-$ Rag1-GFP$^-$ IL-7Rα^- (HSC-enriched), Lin$^-$ IL-7Rα^- c-kit^{hi} Sca-1$^+$ Flt3$^+$ Rag1-GFP$^-$ (LMPP-enriched), Lin$^-$ IL-7Rα^- c-kit^{hi} Sca-1$^+$ Flt3$^+$ Rag1-GFP$^+$ (ELP-enriched), Lin$^-$ c-kit^{lo} Sca-1^{lo} Flt3$^+$ Rag1-GFP$^+$ IL-7Rα^+ (CLP-enriched), and Lin$^-$ c-kit^{hi} Sca-1$^-$ IL-7Rα^- myeloid progenitors (Adolfsson et al., 2005; Igarashi et al., 2002; Kondo et al., 1997). For culture experiments, we also sorted a HSC-enriched fraction from WT C57BL/6 or *Satb1*$^{-/-}$ mice according to the cell surface phenotype of Lin$^-$ c-kit^{hi} Sca-1$^+$ Flt3$^-$.

Stromal Cell Coculture

Murine stromal cell lines MS5 and OP9 were generous gifts from Dr. Mori (Niigata University) and Dr. Hayashi (Tottori University), respectively. Freshly

isolated or transduced cells were cocultured with stromal cells in α-MEM supplemented with 10% FCS, rm SCF (10 ng/mL), rm Flt3-ligand (20 ng/mL), and rm IL-7 (1 ng/mL). The cultures were fed twice a week and maintained for the indicated periods in each experiment. OP9-DL1 cells originated by Dr. Kawamoto (Riken, Japan) were obtained from Riken Cell Bank (Tsukuba, Japan) and used to produce T-lineage cells. In this case, cells were cultured in the presence of rm Flt3-ligand (5 ng/mL) and rm IL-7 (1ng/mL) for 14 days, and rm Flt3-ligand (5 ng/mL) alone thereafter. At the end of culture, cells were counted and analyzed by flow cytometry.

Competitive Repopulation Assay

The CD45.1/CD45.2 system was adapted to a competitive repopulation assay. One thousand Flt3$^-$ LSK cells sorted from FL or BM of WT, Satb1 heterodeficient, or Satb1 homozygous-deficient mice (CD45.2) were mixed with 4×10^5 unfractionated adult BM cells obtained from WT C57BL/6-Ly5.1 (CD45.1) mice and were transplanted into C57BL/6-Ly5.1 mice lethally irradiated at a dose of 920 rad. At 8 weeks after transplantation, engraftment of CD45.2 cells was evaluated by flow cytometry.

Retrovirus Transfection

Murine Satb1 expression vector was purchased from OriGene (Rockville, MD). A retrovirus expression vector for Satb1 was generated by subcloning into the pMYs-IRES-GFP or DsRed vector (a gift from Dr. Kitamura, University of Tokoyo). Conditioned medium containing high tighter retrovirus particles was prepared as reported previously (Satoh et al., 2008). Sorted HSC were cultured in D-MEM containing 10% FBS, rm SCF (100 ng/ml), rm TPO (100 ng/ml), and rm Flt3-ligand (100 ng/ml) for 24 hr. Then, the cells were seeded into the culture plates coated with Retronectin (Takara Bio, Shiga, Japan) and cultured with conditioned medium containing retrovirus. After 24 hr, cells were washed and performed second transfection by the same condition. After 48 hr from the second transfection, GFP or DsRed-positive cells were sorted by FACSaria.

Limiting Dilution Assays

The frequencies of lymphohematopoietic progenitors were determined by plating cells in limiting dilution assays by using 96-well flat-bottom plates. Pre-established MS5 layers were plated with 1, 2, 4, 8, or 16 cells each by using the Automated Cell Deposition Unit of the FACSaria. Cells were cultured in α-MEM supplemented with 10% FCS, rm SCF (10 ng/mL), rm Flt3-ligand (20 ng/mL), and rm IL-7 (1 ng/mL). At 10 days of culture, wells were inspected for the presence of hematopoietic clones. Positive wells were harvested and analyzed by flow cytometry for the presence of CD45$^+$ hematopoietic cells and CD45R/B220$^+$ CD19$^+$ Mac1$^-$ B-lineage cells. The frequencies of progenitors were calculated by linear regression analysis on the basis of Poisson distribution as the reciprocal of the concentration of test cells that gave 37% negative cultures.

Lymphocyte Development from Murine ESCs

To induce differentiation toward hematopoietic cells, we deprived E14tg2a ESCs of leukemia inhibitory factor and seeded onto OP9 cells in 6-well plates at a density of 10^4 cells per well in α-MEM supplemented with 20% FBS (Nakano et al., 1994). After 4.5 days, the cells were harvested and whole-cell suspensions were transferred into a new 10 cm dish and incubated in 37°C for 30 min to remove adherent OP9 cells. The collected floating cells were infected with the retroviral supernatant in Retronectin-coated plates by 2 hr spinoculation (1100 *g*) (Kitajima et al., 2006). Subsequently, the cells were cultured on OP9 or OP9-DL1.

Tetracycline-Regulated Inducible Expression of Satb1 in ESCs

To inducibly express Satb1 in ESCs, we utilized a Tet-off system as reported previously (Era and Witte, 2000), in which transcription of the target gene is initiated by the removal of Tet from the culture medium. Briefly, we initially introduced pCAG20-1-tTA and pUHD10-3-puro by electroporation and selected one clone designated E14 by culture with 1 μg/ml of Puro and/or 1 μg/ml of Tet. We further transfected pUHD10–3-Satb1-GFP, which can inducibly express Satb1 and GFP as a single mRNA through the internal ribosome entry site in response to the Tet removal, together with the neomycin-resistant plasmid pcDNA3.1-neo. After the culture with G418, we selected clones that can inducibly express GFP in response to the Tet deprivation.

DNA PCR Assays for *Igh* Rearrangement

DNA PCR assays were performed as reported previously (Schlissel et al., 1991). PCR was performed by using genomic DNA extracted from splenocytes or ES-derived cells as a template. D_H-J_H recombination was detected as amplified fragments of 1,033 bp, 716 bp, and 333 bp by using a primer $D_HL(5')$ and J3(3′). Germline alleles were detected as an amplified fragment of 1,259 bp by using a primer Mu0(5′) and J3(3′). The sequence of primers are as follows: $D_HL(5')$, GGAATTCG(AorC)TTTTTGT(CorG)AAGGGATCTACTA CTGTG; Mu0(5′), CCGCATGCCAAGGCTAGCCTGAAAGATTACC; and J3(3′), GTCTAGATTCTCACAAGAGTCCGATAGACCCTGG.

Statistical Analyses

Unpaired, two-tailed t test analyses were used for intergroup comparisons, and p values were considered significant if they were less than 0.05.

ACCESSION NUMBERS

The microarray data in Tables S2 and S3 has been deposited in NCBI GEO database under the accession numbers GSE45566 and GSE45299.

SUPPLEMENTAL INFORMATION

Supplemental Information includes four figures, three tables, and Supplemental Experimental Procedures and can be found with this article online at http://dx.doi.org/10.1016/j.immuni.2013.05.014.

ACKNOWLEDGMENTS

We thank T. Nakano for discussion of the results. This work was supported in part by a grant from Mitsubishi Pharma Research Foundation and grants AI020069, HL107138-03, and R37 CA039681 from the National Institutes of Health.

Received: August 30, 2011
Accepted: March 6, 2013
Published: June 20, 2013

REFERENCES

Adolfsson, J., Månsson, R., Buza-Vidas, N., Hultquist, A., Liuba, K., Jensen, C.T., Bryder, D., Yang, L., Borge, O.J., Thoren, L.A., et al. (2005). Identification of Flt3+ lympho-myeloid stem cells lacking erythro-megakaryocytic potential a revised road map for adult blood lineage commitment. Cell *121*, 295–306.

Alvarez, J.D., Yasui, D.H., Niida, H., Joh, T., Loh, D.Y., and Kohwi-Shigematsu, T. (2000). The MAR-binding protein SATB1 orchestrates temporal and spatial expression of multiple genes during T-cell development. Genes Dev. *14*, 521–535.

Cai, S., Han, H.J., and Kohwi-Shigematsu, T. (2003). Tissue-specific nuclear architecture and gene expression regulated by SATB1. Nat. Genet. *34*, 42–51.

Cai, S., Lee, C.C., and Kohwi-Shigematsu, T. (2006). SATB1 packages densely looped, transcriptionally active chromatin for coordinated expression of cytokine genes. Nat. Genet. *38*, 1278–1288.

Chambers, S.M., Shaw, C.A., Gatza, C., Fisk, C.J., Donehower, L.A., and Goodell, M.A. (2007). Aging hematopoietic stem cells decline in function and exhibit epigenetic dysregulation. PLoS Biol. *5*, e201.

Dias, S., Månsson, R., Gurbuxani, S., Sigvardsson, M., and Kee, B.L. (2008). E2A proteins promote development of lymphoid-primed multipotent progenitors. Immunity *29*, 217–227.

Dickinson, L.A., Joh, T., Kohwi, Y., and Kohwi-Shigematsu, T. (1992). A tissue-specific MAR/SAR DNA-binding protein with unusual binding site recognition. Cell *70*, 631–645.

Dobreva, G., Dambacher, J., and Grosschedl, R. (2003). SUMO modification of a novel MAR-binding protein, SATB2, modulates immunoglobulin mu gene expression. Genes Dev. *17*, 3048–3061.

Era, T., and Witte, O.N. (2000). Regulated expression of P210 Bcr-Abl during embryonic stem cell differentiation stimulates multipotential progenitor expansion and myeloid cell fate. Proc. Natl. Acad. Sci. USA *97*, 1737–1742.

Forsberg, E.C., Prohaska, S.S., Katzman, S., Heffner, G.C., Stuart, J.M., and Weissman, I.L. (2005). Differential expression of novel potential regulators in hematopoietic stem cells. PLoS Genet. *1*, e28.

Han, H.J., Russo, J., Kohwi, Y., and Kohwi-Shigematsu, T. (2008). SATB1 reprogrammes gene expression to promote breast tumour growth and metastasis. Nature *452*, 187–193.

Herrscher, R.F., Kaplan, M.H., Lelsz, D.L., Das, C., Scheuermann, R., and Tucker, P.W. (1995). The immunoglobulin heavy-chain matrix-associating regions are bound by Bright: a B cell-specific trans-activator that describes a new DNA-binding protein family. Genes Dev. *9*, 3067–3082.

Igarashi, H., Gregory, S.C., Yokota, T., Sakaguchi, N., and Kincade, P.W. (2002). Transcription from the RAG1 locus marks the earliest lymphocyte progenitors in bone marrow. Immunity *17*, 117–130.

Ikawa, T., Kawamoto, H., Goldrath, A.W., and Murre, C. (2006). E proteins and Notch signaling cooperate to promote T cell lineage specification and commitment. J. Exp. Med. *203*, 1329–1342.

Keren, Z., Naor, S., Nussbaum, S., Golan, K., Itkin, T., Sasaki, Y., Schmidt-Supprian, M., Lapidot, T., and Melamed, D. (2011). B-cell depletion reactivates B lymphopoiesis in the BM and rejuvenates the B lineage in aging. Blood *117*, 3104–3112.

Kitajima, K., Tanaka, M., Zheng, J., Yen, H., Sato, A., Sugiyama, D., Umehara, H., Sakai, E., and Nakano, T. (2006). Redirecting differentiation of hematopoietic progenitors by a transcription factor, GATA-2. Blood *107*, 1857–1863.

Kondo, M., Weissman, I.L., and Akashi, K. (1997). Identification of clonogenic common lymphoid progenitors in mouse bone marrow. Cell *91*, 661–672.

Kuwata, N., Igarashi, H., Ohmura, T., Aizawa, S., and Sakaguchi, N. (1999). Cutting edge: absence of expression of RAG1 in peritoneal B-1 cells detected by knocking into RAG1 locus with green fluorescent protein gene. J. Immunol. *163*, 6355–6359.

Lai, A.Y., and Kondo, M. (2008). T and B lymphocyte differentiation from hematopoietic stem cell. Semin. Immunol. *20*, 207–212.

Medina, K.L., Pongubala, J.M., Reddy, K.L., Lancki, D.W., Dekoter, R., Kieslinger, M., Grosschedl, R., and Singh, H. (2004). Assembling a gene regulatory network for specification of the B cell fate. Dev. Cell *7*, 607–617.

Miller, J.P., and Allman, D. (2005). Linking age-related defects in B lymphopoiesis to the aging of hematopoietic stem cells. Semin. Immunol. *17*, 321–329.

Montecino-Rodriguez, E., and Dorshkind, K. (2006). Evolving patterns of lymphopoiesis from embryogenesis through senescence. Immunity *24*, 659–662.

Nakano, T., Kodama, H., and Honjo, T. (1994). Generation of lymphohematopoietic cells from embryonic stem cells in culture. Science *265*, 1098–1101.

Ng, S.Y., Yoshida, T., Zhang, J., and Georgopoulos, K. (2009). Genome-wide lineage-specific transcriptional networks underscore Ikaros-dependent lymphoid priming in hematopoietic stem cells. Immunity *30*, 493–507.

Notani, D., Gottimukkala, K.P., Jayani, R.S., Limaye, A.S., Damle, M.V., Mehta, S., Purbey, P.K., Joseph, J., and Galande, S. (2010). Global regulator SATB1 recruits beta-catenin and regulates T(H)2 differentiation in Wnt-dependent manner. PLoS Biol. *8*, e1000296.

Oritani, K., Medina, K.L., Tomiyama, Y., Ishikawa, J., Okajima, Y., Ogawa, M., Yokota, T., Aoyama, K., Takahashi, I., Kincade, P.W., and Matsuzawa, Y. (2000). Limitin: An interferon-like cytokine that preferentially influences B-lymphocyte precursors. Nat. Med. *6*, 659–666.

Rossi, D.J., Bryder, D., Zahn, J.M., Ahlenius, H., Sonu, R., Wagers, A.J., and Weissman, I.L. (2005). Cell intrinsic alterations underlie hematopoietic stem cell aging. Proc. Natl. Acad. Sci. USA *102*, 9194–9199.

Satoh, Y., Matsumura, I., Tanaka, H., Ezoe, S., Fukushima, K., Tokunaga, M., Yasumi, M., Shibayama, H., Mizuki, M., Era, T., et al. (2008). AML1/RUNX1 works as a negative regulator of c-Mpl in hematopoietic stem cells. J. Biol. Chem. *283*, 30045–30056.

Savarese, F., Dávila, A., Nechanitzky, R., De La Rosa-Velazquez, I., Pereira, C.F., Engelke, R., Takahashi, K., Jenuwein, T., Kohwi-Shigematsu, T., Fisher, A.G., and Grosschedl, R. (2009). Satb1 and Satb2 regulate embryonic stem cell differentiation and Nanog expression. Genes Dev. *23*, 2625–2638.

Schlissel, M.S., Corcoran, L.M., and Baltimore, D. (1991). Virus-transformed pre-B cells show ordered activation but not inactivation of immunoglobulin gene rearrangement and transcription. J. Exp. Med. *173*, 711–720.

Scott, E.W., Fisher, R.C., Olson, M.C., Kehrli, E.W., Simon, M.C., and Singh, H. (1997). PU.1 functions in a cell-autonomous manner to control the differentiation of multipotential lymphoid-myeloid progenitors. Immunity *6*, 437–447.

Semerad, C.L., Mercer, E.M., Inlay, M.A., Weissman, I.L., and Murre, C. (2009). E2A proteins maintain the hematopoietic stem cell pool and promote the maturation of myelolymphoid and myeloerythroid progenitors. Proc. Natl. Acad. Sci. USA *106*, 1930–1935.

Shimazu, T., Iida, R., Zhang, Q., Welner, R.S., Medina, K.L., Alberola-Lla, J., and Kincade, P.W. (2012). CD86 is expressed on murine hematopoietic stem cells and denotes lymphopoietic potential. Blood *119*, 4889–4897.

Sudo, K., Ema, H., Morita, Y., and Nakauchi, H. (2000). Age-associated characteristics of murine hematopoietic stem cells. J. Exp. Med. *192*, 1273–1280.

Yang, Q., Kardava, L., St Leger, A., Martincic, K., Varnum-Finney, B., Bernstein, I.D., Milcarek, C., and Borghesi, L. (2008). E47 controls the developmental integrity and cell cycle quiescence of multipotential hematopoietic progenitors. J. Immunol. *181*, 5885–5894.

Yasui, D., Miyano, M., Cai, S., Varga-Weisz, P., and Kohwi-Shigematsu, T. (2002). SATB1 targets chromatin remodelling to regulate genes over long distances. Nature *419*, 641–645.

Yilmaz, O.H., Kiel, M.J., and Morrison, S.J. (2006). SLAM family markers are conserved among hematopoietic stem cells from old and reconstituted mice and markedly increase their purity. Blood *107*, 924–930.

Yokota, T., Kouro, T., Hirose, J., Igarashi, H., Garrett, K.P., Gregory, S.C., Sakaguchi, N., Owen, J.J., and Kincade, P.W. (2003a). Unique properties of fetal lymphoid progenitors identified according to RAG1 gene expression. Immunity *19*, 365–375.

Yokota, T., Meka, C.S., Kouro, T., Medina, K.L., Igarashi, H., Takahashi, M., Oritani, K., Funahashi, T., Tomiyama, Y., Matsuzawa, Y., and Kincade, P.W. (2003b). Adiponectin, a fat cell product, influences the earliest lymphocyte precursors in bone marrow cultures by activation of the cyclooxygenase-prostaglandin pathway in stromal cells. J. Immunol. *171*, 5091–5099.

Yokota, T., Oritani, K., Garrett, K.P., Kouro, T., Nishida, M., Takahashi, I., Ichii, M., Satoh, Y., Kincade, P.W., and Kanakura, Y. (2008). Soluble frizzled-related protein 1 is estrogen inducible in bone marrow stromal cells and suppresses the earliest events in lymphopoiesis. J. Immunol. *181*, 6061–6072.

Yoshida, T., Ng, S.Y., Zuniga-Pflucker, J.C., and Georgopoulos, K. (2006). Early hematopoietic lineage restrictions directed by Ikaros. Nat. Immunol. *7*, 382–391.

Mise et al. BMC Nephrology 2013, 14:156
http://www.biomedcentral.com/1471-2369/14/156

BMC Nephrology

CASE REPORT Open Access

Long term follow up of congenital thrombotic thrombocytopenic purpura (Upshaw-Schulman syndrome) on hemodialysis for 19 years: a case report

Koki Mise[1,6*], Yoshifumi Ubara[1,3,6], Masanori Matsumoto[4], Keiichi Sumida[1,6], Rikako Hiramatsu[1], Eiko Hasegawa[1], Masayuki Yamanouchi[1], Noriko Hayami[1,6], Tatsuya Suwabe[1,6], Junichi Hoshino[1,6], Naoki Sawa[1], Kenichi Ohashi[2], Koichi Kokame[5], Toshiyuki Miyata[5], Yoshihiro Fujimura[4] and Kenmei Takaichi[1,3]

Abstract

Background: Thrombotic thrombocytopenic purpura (TTP) is frequently associated with renal abnormalities, but there have been few reports about renal abnormalities in patients with hereditary TTP. In particular, little is known about the long-term prognosis of patients with childhood-onset congenital TTP.

Case presentation: We report a Japanese patient with congenital TTP (Upshaw–Schulman syndrome) who was followed for 19 years after initiation of hemodialysis when he was 22 years old. At the age of 6 years, the first episode of purpura, thrombocytopenia, and proteinuria occurred without any precipitating cause. He underwent living-related donor kidney transplantation from his mother, but the graft failed after 5 months due to recurrence of TTP. Even after resection of the transplanted kidney and resumption of regular hemodialysis, TTP became refractory to infusion of fresh frozen plasma (FFP). Therefore, splenectomy was performed and his disease remained in remission for 10 years. However, TTP recurred at the age of 39 years. Plasma activity of ADAMTS13 (a disintegrin and metalloprotease with thrombospondin type I domain 13) was less than 3%, while ADAMTS13 inhibitor was not detected (< 0.5 Bethesda units/mL). The patient died suddenly after hemodialysis at the age of 41 years. Subsequent genetic analysis of this patient and his parents revealed two different heterozygous mutations of ADAMTS13, including a missense mutation in exon 26 (c.3650T>C causing p.I1217T) inherited from his father and a missense mutation in exon 21 (c.2723G>A causing p.C908Y) inherited from his mother. The former mutation has not been detected before in Japan, while the latter mutation is common in Japan. A retrospective review showed that serum C3 levels were consistently low while C4 levels were normal during follow-up, and C3 decreased much further during each episode of TTP.

Conclusion: Congenital TTP was diagnosed from the clinical, biochemical, and genetic findings. Infusion of FFP controlled each thrombotic episode, but the effect was limited and of short duration. Review of the complement profile in this patient suggested that a persistently low serum C3 level might be associated with refractory TTP and a worse renal prognosis.

Keywords: Congenital thrombotic thrombocytopenic purpura, ADAMTS13 (a disintegrin and metalloprotease with thrombospondin type I domain 13), Chronic hemodialysis, Complement activation, C3, Alternative pathway

* Correspondence: kokims-frz@umin.ac.jp
[1]Nephrology Center, Toranomon Hospital, Tokyo, Japan
[6]Nephrology Center, Toranomon Hospital Kajigaya, 1-3-1, Kajigaya, Takatu-ku, Kawasaki-shi, Kanagawa-ken 213-0015, Japan
Full list of author information is available at the end of the article

Background

Thrombotic thrombocytopenic purpura (TTP) is a rare disorder characterized by thrombocytopenia and microangiopathic hemolytic anemia. Congenital TTP has been reported to be associated with severe deficiency of the plasma activity of ADAMTS13 (a disintegrin and metalloprotease with thrombospondin type I domain 13), which is reduced to <5% of normal by mutation of the ADAMTS13 gene, and this is known as the Upshaw–Schulman syndrome (USS) [1,2]. Deficiency of ADAMTS13 activity can also be caused by inhibitory antibodies targeting ADAMTS13, leading to acquired TTP. ADAMTS13 is a metalloproteinase that specifically cleaves multimeric von Willebrand factor (VWF) [2], while VWF is a large glycoprotein that is essential for platelet adhesion and aggregation under high shear stress conditions [3]. ADAMTS13 is mainly synthesized in the liver by stellate cells [4,5]. In addition, it is expressed by the podocytes and endothelium of the renal glomeruli, where podocyte-derived ADAMTS13 might have a local protective effect in the high shear stress glomerular microcirculation [6].

TTP is often associated with renal abnormalities and there have been some reports about such abnormalities in TTP patients, but few about hereditary TTP. In particular, there is little information about the long-term prognosis of patients with childhood-onset congenital TTP [7]. Here, we report a Japanese man with congenital TTP confirmed by genetic analysis, who was followed up for 19 years after initiation of hemodialysis.

Case presentation

A 22-year-old man was admitted to our hospital for renal transplantation. He was the third of five children of non-consanguineous parents. There was no history of severe neonatal jaundice. Purpura of the lower extremities, thrombocytopenia, and proteinuria occurred without any precipitating cause at the age of 6 years, and hemolytic uremic syndrome (HUS) was diagnosed. This episode subsided spontaneously without treatment, but there were repeated recurrences and his renal function deteriorated gradually. In 1990, at the age of 22 years, hemodialysis was started for end-stage renal disease (ESRD) along with the occurrence of cerebral infarction. After 4 months, living-related kidney transplantation was performed with his mother as the donor. Immunosuppressive therapy included prednisolone (70 mg daily), cyclosporine (420 mg daily), antilymphocyte globulin (1 g daily), and azathioprine (100 mg daily). At 7 days after surgery, he developed thrombocytopenia (23.1 to $1.8 \times 10^4/\mu L$) and hemolytic anemia (Hb: 10.3 to 8.2 g/dL), along with an increase of serum creatinine (1.1 to 2.1 mg/dL), lactate dehydrogenase (LDH: 208 to 785 IU), and total bilirubin (0.4 to 2.2 mg/dL). Haptoglobulin was decreased to 3.4 mg/dL. Serum levels of C3 and C4 were also decreased (C3: 63.0 to 51.7 mg/dL, normal range; 83 to 177 mg/dL, C4: 34.4 to 22.9, normal range; 15 to 45 mg/dL). Activation of HUS was suspected to have been caused by cyclosporine, so it was switched to deoxyspergualin (200 mg daily). After methylprednisolone pulse therapy (500 mg/day for 3 days) and infusion of fresh frozen plasma (FFP) (800 mL × 5 days), HUS subsided temporarily. However, there was frequent relapse of HUS, so azathioprine was changed to mizoribine and muromonab-CD3 was administered. Plasma exchange or infusion FFP was effective for terminating each episode of HUS. After 50 days, cerebral hemorrhage occurred, followed by gastrointestinal bleeding at 90 days. Then HUS recurred with thrombocytopenia and hemolytic anemia, which was refractory to plasma exchange or infusion of FFP, and his renal function deteriorated gradually. In May 1991, removal of the kidney graft was performed and hemodialysis was restarted. Examination of the resected kidney showed thrombi, endothelial cell swelling, and numerous red blood cells in the glomeruli and small arteries (Figure 1). After nephrectomy, jejunal bleeding was treated by transcatheter arterial embolization of an arteriovenous malformation in the superior mesenteric artery territory.

Even after hemodialysis was resumed, transient ischemic attacks and cerebral infarction occurred every time his platelet count decreased spontaneously, subsiding in response to infusion of FFP. However, TTP became refractory to FFP in 1998. Because indium platelet scintigraphy showed high uptake in the spleen and his platelets had a short lifespan (1.76 days), splenectomy was performed in order to prevent excessive platelet destruction. Thereafter, thrombotic episodes requiring the infusion of FFP did not occur for 10 years until 2008. During this remission period, the serum level of C3 was always lower than normal and serum C4 was normal, while the C3 level decreased much further with each episode of TTP. When cerebral infarction with thrombocytopenia occurred again at the age of 39 years, plasma ADAMTS13 activity was less than 5% of normal, as measured by the FRETS-VWF73 assay [8], while ADAMTS13 inhibitor was negative (<0.5 Bethesda units/mL) [9]. USS was diagnosed because he had severe deficiency of ADAMTS13 activity without any detectable inhibitor in conjunction with appropriate clinical criteria. Although the thrombotic episodes subsided following infusion of FFP, he died suddenly after hemodialysis in 2010 at the age of 41 years. After the patient's death, we measured plasma ADAMTS13 activity and inhibitor in his parents using a chromogenic ELISA [10]. Both of them had ADAMTS13 activity around 30% of normal and the inhibitor was negative.

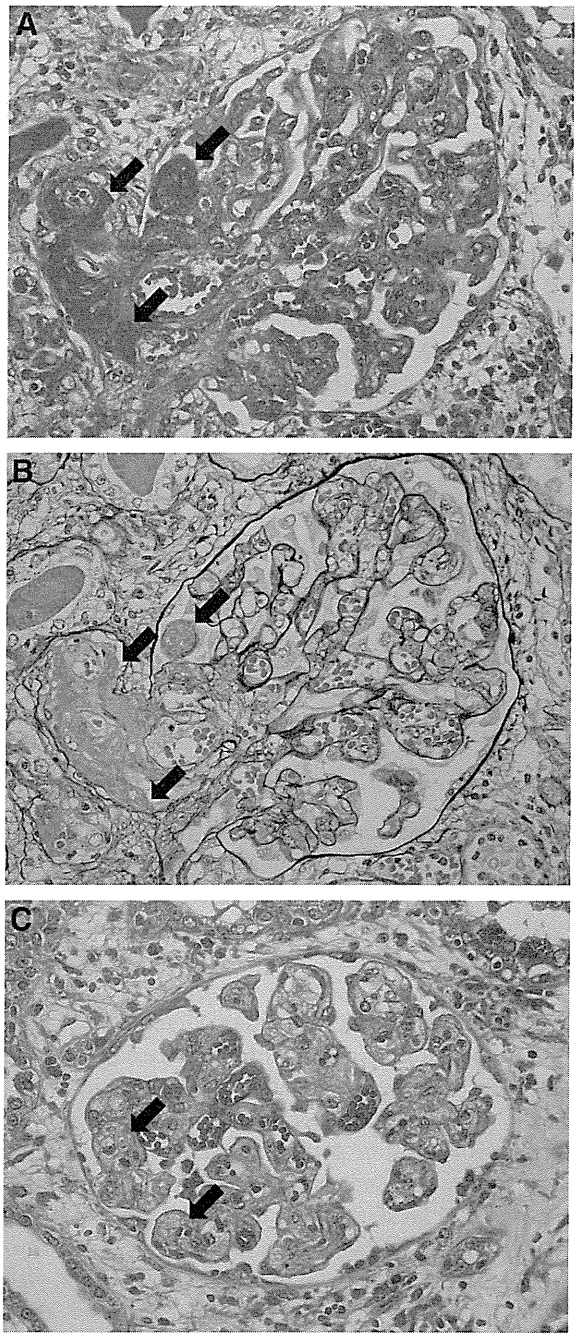

Figure 1 Renal histopathological findings. A, **B**: Fibrin thrombi in small arteries (arrows) and a glomerulus containing numerous red blood cells (**A**: Heidenhain's azan trichrome stain, **B**: Periodic acid methenamine silver stain × 400). **C**: Endothelial cell swelling (arrows) (Heidenhain's azan trichrome stain × 400).

Genetic analysis

After obtaining consent from his parents, genetic analysis of the patient and parents was performed with the approval of the Ethics Committees of Nara Medical University, the National Cerebral and Cardiovascular Center, and Toranomon Hosipital. Genetic analysis of the patient was carried out at the National Cerebral and Cardiovascular Center using DNA extracted from the resected spleen. For his parents, analysis was performed at the Department of Blood Transfusion Medicine of Nara Medical University.

It was demonstrated that the patient had compound heterozygous mutations of ADAMTS13, comprising a missense mutation in exon 26 (c.3650T>C causing p. I1217T) that was inherited from his father and a missense mutation in exon 21 (c.2723G>A causing p.C908Y) inherited from his mother. A diagnosis of congenital TTP (USS) was confirmed by these findings (Figure 2).

Discussion

It is widely recognized that TTP is associated with renal abnormalities, with renal failure occurring secondary to damage caused by microthrombi that develop because of decreased plasma ADAMTS13 activity. The common renal manifestations of TTP are proteinuria and hematuria. Acute renal failure (ARF) affects 11% of patients with severe congenital TTP and often recurs with exacerbation of this disease [7]. Although ARF requiring dialysis was reported to be less frequent (0–9.7%) in four series of patients with acquired TTP [11-13], the percentage of patients with congenital TTP who need regular dialysis is unclear. Tsai et al. [7] reported that five out of nine patients with USS progressed to ESRD requiring dialysis, and three of them had episodes of ARF. Therefore, repeated episodes of ARF may be associated with progression to ESRD.

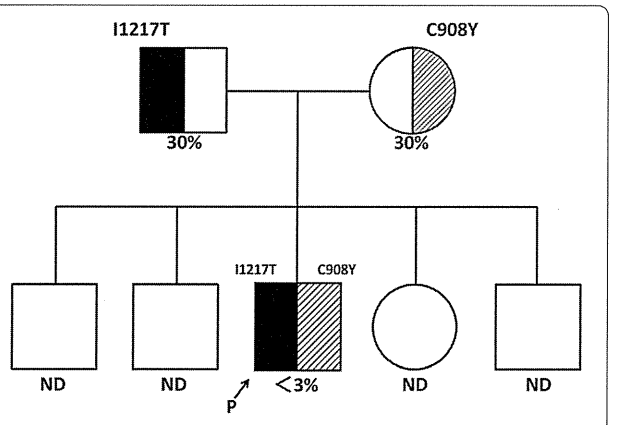

Figure 2 Pedigree of the index patient with genetic haplotypes and plasma activity of ADAMTS13 (a disintegrin and metalloprotease with thrombospondin type I domain 13). Squares represent males and circles represent females. Plasma ADAMTS13 activity (%) is shown under the circles and squares. Mutations of the ADAMTS13 gene are shown as one-letter amino acid abbreviations numbered from the initial Met codon. The arrow indicates the index patient. The mother and father of the index patient are both asymptomatic carriers. Abbreviations P: patient, ND: not determined.

Because infusion of plasma is effective for acute exacerbation of congenital TTP, plasma exchange is the standard treatment. In patients with relapsing and/or refractory TTP, splenectomy can be effective. The mechanism is assumed to be that splenectomy decreases autoantibody production by removing a large reservoir of B lymphocytes [14], which is a reasonable explanation for patients with acquired TTP and elevated levels of ADAMTS13 inhibitor. However, Snider et al. [15] reported a patient with relapsing and refractory congenital TTP who remained in complete clinical remission for 4 years after splenectomy. In our patient, remission of TTP persisted for 10 years after splenectomy, but the effect was limited. The mechanism by which splenectomy improves congenital TTP is unknown, although it is possible that a state like idiopathic thrombocytopenia purpura (ITP) might have coexisted with TTP in our patient because his short platelet lifespan was compatible with ITP. Since TTP remained in remission for 10 years after splenectomy without the need for FFP, this case shows that splenectomy can be a useful option for relapsing/refractory congenital TTP. There has only been one previous case report of renal transplantation for chronic renal failure in a patient with congenital TTP, and the graft showed early failure due to disease recurrence [16]. In our case, the graft also failed due to chronic relapsing TTP only 5 months after transplantation. Therefore, renal transplantation may not a feasible option for ESRD in patients with congenital TTP.

Several mutations of the ADAMTS13 gene have been reported in congenital TTP. It is thought that specific ADAMTS13 mutations are more common among certain ethnicities [17]. Fujimura et al. [17] evaluated 43 USS patients in Japan and found ADAMTS13 mutations that were specific to Japanese individuals with congenital TTP. The present patient had p.C908Y with maternal inheritance, which is one of the common ADAMTS13 mutations found in Japanese patients [17]. However, the patient also had p.I1271T (inherited from his father) and this has not been reported before in Japanese patients, was although it is consistent with the missense mutation reported by Park et al. [18] in a Korean patient who had congenital TTP complicating moyamoya disease. Fujimura et al. [17] reported that two out of 43 patients with congenital TTP progressed to ESRD requiring dialysis. One of them was homozygous for c.414 + 1G > A, while the other was heterozygous for c.1885delT (paternal inheritance) and p.C908Y (maternal inheritance). However, these mutations were also detected in some of their TTP patients without progression to dialysis. In fact, five of the 43 patients had the p.C908Y mutation that was detected in our case, but only one of them progressed to dialysis during follow-up. Therefore, as Tsai et al. [7] concluded, the relation between ADAMTS13 mutation and the renal prognosis remains uncertain [17].

With regard to the occurrence of renal impairment in this patient, it may be important to focus on the complement system. Ruiz-Torres et al. [19] studied thrombotic microangiopathy patients with congenital ADAMTS13 deficiency and patients with ADAMTS 13 inhibitors, and they reported that four of out of six patients (66%) showed a moderate decrease of C3 in the acute phase, which was indicative of complement activation and consumption. They hypothesized that platelet microthrombi caused activation of the alternative pathway in patients with ADAMTS13 deficiency. Moreover, Noris et al. [20] reported 2 sisters who had the same compound heterozygous ADAMTS13 mutations, while one sister also had a heterozygous mutation of the gene encoding complement factor H, a plasma factor that inhibits activation of the alternative pathway. The second sister had severe disease, with renal involvement requiring chronic dialysis, and eventually died of a stroke. She had subnormal serum C3 levels and normal C4 levels. In addition, one of the four congenital TTP patients reported by Ruiz-Torres et al. had a subnormal C3 level even in remission and her serum creatinine level was 5.73 mg/dL, suggesting ESRD. Considering these reports, some patients with congenital TTP may have persistently low C3 levels that may be associated with a worse renal prognosis. The findings in our case seem to support this hypothesis. If a persistently depressed C3 level and normal C4 level, indicating selective activation of the alternative pathway, is one of the causes of severe TTP, the anti-C5 monoclonal antibody eculizumab may be an effective treatment for refractory TTP. In fact, Chapin et al. [21] reported that eculizumab was effective for refractory TTP, so use of eculizumab might have been a good treatment option in our case.

Conclusion

We encountered a male patient with congenital TTP who remained on hemodialysis for 19 years. His ADAMTS13 gene had two mutations, which were p.I1217T (the first report of this mutation in Japan) and p.C908Y (common in Japan). Infusion of FFP was effective for controlling thrombotic episodes, but the improvement was limited and of short duration. The profile of complement components in this patient suggests an association of persistently low serum C3 level with refractory TTP and a worse renal prognosis.

Consent

Written informed consent was obtained from the patient's parents for the genetic analyses, as well as for publication of this case report and any accompanying images. We could not obtain written consent from the patient himself because he was already dead when we wrote this paper.

Competing interests
The authors declare that they have no competing interests.

Authors' contributions
KM contributed to analyzing and interpretation of data and writing the manuscript. YU contributed to analyzing and interpretation of data and writing the manuscript. MM contributed to analyzing and interpretation of data and writing the manuscript. KS contributed to managing the patient and assessing data. RH contributed to managing the patient and assessing data. EH contributed to managing the patient and assessing data. MY contributed to managing the patient and assessing data. NH contributed to managing the patient and assessing data. TS contributed to managing the patient and assessing data. JH contributed to managing the patient and assessing data. NS contributed to managing the patient and assessing data. KO contributed to analyzing and interpretation of pathological findings. KK contributed to analyzing the ADAMTS13 gene of patient. TM contributed to analyzing the ADAMTS13 gene of patient. YF contributed to analyzing and interpretation of data and writing the manuscript. KT contributed to analyzing and interpretation of data and management the patient. All authors read and approved the final manuscript.

Acknowledgements
This work was partly supported by a grant from the Okinaka Memorial Institute for Medical Research and by grants-in-aid from the Ministry of Health, Labor, and Welfare of Japan; the Ministry of Education, Culture, Sports, Science, and Technology of Japan; the Japan Society for the Promotion of Science; and Takeda Medical Foundation of Japan.

Author details
[1]Nephrology Center, Toranomon Hospital, Tokyo, Japan. [2]Department of Pathology, Toranomon Hospital, Tokyo, Japan. [3]Okinaka Memorial Institute for Medical Research, Toranomon Hospital, Tokyo, Japan. [4]Department of Blood Transfusion Medicine, Nara Medical University, Nara, Japan. [5]Department of Molecular Pathogenesis, National Cerebral and Cardiovascular Center, Suita, Osaka, Japan. [6]Nephrology Center, Toranomon Hospital Kajigaya, 1-3-1, Kajigaya, Takatu-ku, Kawasaki-shi, Kanagawa-ken 213-0015, Japan.

Received: 8 March 2013 Accepted: 9 July 2013
Published: 20 July 2013

References

1. Bianchi V, Robles R, Alberio L, Furlan M, Lammle B: **Von willebrand factor-cleaving protease (ADAMTS13) in thrombocytopenic disorders: a severely deficient activity is specific for thrombotic thrombocytopenic purpura.** *Blood* 2002, **100**(2):710–713.
2. Levy GG, Nichols WC, Lian EC, Foroud T, McClintick JN, McGee BM, Yang AY, Siemieniak DR, Stark KR, Gruppo R, *et al*: **Mutations in a member of the ADAMTS gene family cause thrombotic thrombocytopenic purpura.** *Nature* 2001, **413**(6855):488–494.
3. Ruggeri ZM: **Structure and function of von willebrand factor.** *Thromb Haemost* 1999, **82**(2):576–584.
4. Uemura M, Tatsumi K, Matsumoto M, Fujimoto M, Matsuyama T, Ishikawa M, Iwamoto TA, Mori T, Wanaka A, Fukui H, *et al*: **Localization of ADAMTS13 to the stellate cells of human liver.** *Blood* 2005, **106**(3):922–924.
5. Zhou W, Inada M, Lee TP, Benten D, Lyubsky S, Bouhassira EE, Gupta S, Tsai HM: **ADAMTS13 Is expressed in hepatic stellate cells.** *Lab Invest* 2005, **85**(6):780–788.
6. Manea M, Kristoffersson A, Schneppenheim R, Saleem MA, Mathieson PW, Morgelin M, Bjork P, Holmberg L, Karpman D: **Podocytes express ADAMTS13 in normal renal cortex and in patients with thrombotic thrombocytopenic purpura.** *Br J Haematol* 2007, **138**(5):651–662.
7. Tsai HM: **The kidney in thrombotic thrombocytopenic purpura.** *Minerva Med* 2007, **98**(6):731–747.
8. Kokame K, Nobe Y, Kokubo Y, Okayama A, Miyata T: **FRETS-VWF73, a first fluorogenic substrate for ADAMTS13 assay.** *Br J Haematol* 2005, **129**(1):93–100.
9. Furlan M, Robles R, Galbusera M, Remuzzi G, Kyrle PA, Brenner B, Krause M, Scharrer I, Aumann V, Mittler U, *et al*: **von willebrand factor-cleaving protease in thrombotic thrombocytopenic purpura and the hemolytic-uremic syndrome.** *N Engl J Med* 1998, **339**(22):1578–1584.
10. Kato S, Matsumoto M, Matsuyama T, Isonishi A, Hiura H, Fujimura Y: **Novel monoclonal antibody-based enzyme immunoassay for determining plasma levels of ADAMTS13 activity.** *Transfusion* 2006, **46**(8):1444–1452.
11. Vesely SK, George JN, Lammle B, Studt JD, Alberio L, El-Harake MA, Raskob GE: **ADAMTS13 Activity in thrombotic thrombocytopenic purpura-hemolytic uremic syndrome: relation to presenting features and clinical outcomes in a prospective cohort of 142 patients.** *Blood* 2003, **102**(1):60–68.
12. Raife T, Atkinson B, Montgomery R, Vesely S, Friedman K: **Severe deficiency of VWF-cleaving protease (ADAMTS13) activity defines a distinct population of thrombotic microangiopathy patients.** *Transfusion* 2004, **44**(2):146–150.
13. Zheng XL, Kaufman RM, Goodnough LT, Sadler JE: **Effect of plasma exchange on plasma ADAMTS13 metalloprotease activity, inhibitor level, and clinical outcome in patients with idiopathic and nonidiopathic thrombotic thrombocytopenic purpura.** *Blood* 2004, **103**(11):4043–4049.
14. Bouw MC, Dors N, van Ommen H, Ramakers-van Woerden NL: **Thrombotic thrombocytopenic purpura in childhood.** *Pediatr Blood Cancer* 2009, **53**(4):537–542.
15. Snider CE, Moore JC, Warkentin TE, Finch CN, Hayward CP, Kelton JG: **Dissociation between the level of von willebrand factor-cleaving protease activity and disease in a patient with congenital thrombotic thrombocytopenic purpura.** *Am J Hematol* 2004, **77**(4):387–390.
16. Veyradier A, Lavergne JM, Ribba AS, Obert B, Loirat C, Meyer D, Girma JP: **Ten candidate ADAMTS13 mutations in six french families with congenital thrombotic thrombocytopenic purpura (upshaw-schulman syndrome).** *J Thromb Haemost* 2004, **2**(3):424–429.
17. Fujimura Y, Matsumoto M, Isonishi A, Yagi H, Kokame K, Soejima K, Murata M, Miyata T: **Natural history of upshaw-schulman syndrome based on ADAMTS13 gene analysis in Japan.** *J Thromb Haemost* 2011, **9**(Suppl 1):283–301.
18. Park HW, Oh D, Kim N, Cho HY, Moon KC, Chae JH, Ahn HS, Choi Y, Cheong HI: **Congenital thrombotic thrombocytopenic purpura associated with unilateral moyamoya disease.** *Pediatr Nephrol* 2008, **23**(9):1555–1558.
19. Ruiz-Torres MP, Casiraghi F, Galbusera M, Macconi D, Gastoldi S, Todeschini M, Porrati F, Belotti D, Pogliani EM, Noris M, *et al*: **Complement activation: the missing link between ADAMTS-13 deficiency and microvascular thrombosis of thrombotic microangiopathies.** *Thromb Haemost* 2005, **93**(3):443–452.
20. Noris M, Bucchioni S, Galbusera M, Donadelli R, Bresin E, Castelletti F, Caprioli J, Brioschi S, Scheiflinger F, Remuzzi G: **Complement factor H mutation in familial thrombotic thrombocytopenic purpura with ADAMTS13 deficiency and renal involvement.** *J Am Soc Nephrol* 2005, **16**(5):1177–1183.
21. Chapin J, Weksler B, Magro C, Laurence J: **Eculizumab in the treatment of refractory idiopathic thrombotic thrombocytopenic purpura.** *Br J Haematol* 2012, **157**(6):772–774.

doi:10.1186/1471-2369-14-156
Cite this article as: Mise *et al.*: Long term follow up of congenital thrombotic thrombocytopenic purpura (Upshaw-Schulman syndrome) on hemodialysis for 19 years: a case report. *BMC Nephrology* 2013 **14**:156.

PLOS ONE

A Deficiency of Herp, an Endoplasmic Reticulum Stress Protein, Suppresses Atherosclerosis in ApoE Knockout Mice by Attenuating Inflammatory Responses

Shohei Shinozaki[1], Tsuyoshi Chiba[1,2], Koichi Kokame[3], Toshiyuki Miyata[3], Eiji Kaneko[1], Kentaro Shimokado[1]*

1 Geriatrics and Vascular Medicine, Tokyo Medical and Dental University Graduate School, Tokyo, Japan, **2** Information Center, National Institute of Health and Nutrition, Tokyo, Japan, **3** Department of Molecular Pathogenesis, National Cerebral and Cardiovascular Center, Osaka, Japan

Abstract

Herp was originally identified as an endoplasmic reticulum (ER) stress protein in vascular endothelial cells. ER stress is induced in atherosclerotic lesions, but it is not known whether Herp plays any role in the development of atherosclerosis. To address this question, we generated Herp- and apolipoprotein E (apoE)-deficient mice (Herp$^{-/-}$; apoE$^{-/-}$ mice) by crossbreeding Herp$^{-/-}$ mice and apoE$^{-/-}$ mice. Herp was expressed in the endothelial cells and medial smooth muscle cells of the aorta, as well as in a subset of macrophages in the atherosclerotic lesions in apoE$^{-/-}$ mice, while there was no expression of Herp in the Herp$^{-/-}$; apoE$^{-/-}$ mice. The doubly deficient mice developed significantly fewer atherosclerotic lesions than the apoE$^{-/-}$ mice at 36 and 72 weeks of age, whereas the plasma levels of cholesterol and triglycerides were not significantly different between the strains. The plasma levels of non-esterified fatty acids were significantly lower in the Herp$^{-/-}$; apoE$^{-/-}$ mice when they were eight and 16 weeks old. The gene expression levels of ER stress response proteins (GRP78 and CHOP) and inflammatory cytokines (IL-1β, IL-6, TNF-α and MCP-1) in the aorta were significantly lower in Herp$^{-/-}$; apoE$^{-/-}$ mice than in apoE$^{-/-}$ mice, suggesting that Herp mediated ER stress-induced inflammation. In fact, peritoneal macrophages isolated from Herp-deficient mice and RAW264.7 macrophages in which Herp was eliminated with a siRNA expressed lower levels of mRNA for inflammatory cytokines when they were treated with tunicamycin. Herp deficiency affected the major mediators of the unfolded protein response, including IRE1 and PERK, but not ATF6. These findings suggest that a deficiency of Herp suppressed the development of atherosclerosis by attenuating the ER stress-induced inflammatory reactions.

Citation: Shinozaki S, Chiba T, Kokame K, Miyata T, Kaneko E, et al. (2013) A Deficiency of Herp, an Endoplasmic Reticulum Stress Protein, Suppresses Atherosclerosis in ApoE Knockout Mice by Attenuating Inflammatory Responses. PLoS ONE 8(10): e75249. doi:10.1371/journal.pone.0075249

Editor: Ryuichi Morishita, Osaka University Graduate School of Medicine, Japan

Received March 7, 2013; **Accepted** August 13, 2013; **Published** October 28, 2013

Funding: This study was supported by a grant to KS from Ministry of Education, Culture, Sports, Science and Technology. The funders had no role in study design, data collection and analysis, decision to publish, or preparation of the manuscript.

Competing Interests: TM is a PLOS ONE Editorial Board member, however, he has no conflict of interest with regard to this manuscript. This does not alter the authors' adherence to all the PLOS ONE policies on sharing data and materials.

* E-mail: k.shimoka.vasc@tmd.ac.jp

Introduction

There has been an increasing number of reports on endoplasmic reticulum (ER) stress in atherosclerotic lesion. Markers of ER stress and activation of the unfolded protein responses (UPR) are observed at all stages of atherosclerotic lesions, particularly in macrophages [1–3]. Lipid accumulation and disturbances in calcium homeostasis induce ER stress, the UPR and ER-associated degradation (ERAD) [4–6]. ER stress is an important event during the initiation, progression and clinical progression of atherosclerosis [3]. At an early stage of atherosclerosis, the increased number of apoptotic cells in macrophages suppresses early atherosclerotic lesion development [7]. ER stress-related proteins, such as glucose regulate protein 78 (GRP78) and C/EBP homologous protein (CHOP) are expressed in macrophage-derived foam cells [1]. At advanced stages, ER stress causes the apoptosis of macrophages, thus increasing the necrotic core size, and elicits inflammatory reactions [8].

The relationship between ER stress and inflammation has gradually been revealed. ER stress stimulates three distinct UPR-signaling pathways through sensors that include protein kinase-like ER kinase (PERK), inositol-requiring transmembrane kinase and endonuclease 1 (IRE1α) and activation of transcription factor 6 (ATF6). The PERK–CHOP pathway has been extensively investigated, and CHOP plays a central role in the inflammatory response and apoptosis of macrophages. CHOP deficiency prevents the development of atherosclerosis by reducing apoptosis and inflammation in the arteries of apoE$^{-/-}$ mice [9]. It has been reported that the activation of NF-κB pathway occurs via the ATF-6 branch [10,11].

Herp is an ER stress-associated protein that was originally found as a gene product that was upregulated in vascular endothelial cells treated with homocysteine [12]. It is ubiquitously expressed in various tissues and organs, and is highly expressed in the heart, liver, skeletal muscle, kidneys and pancreas [12]. Herp is dually regulated by shared (PERK/eIF-2alpha dependent) and the ER stress-specific (IRE1/XBP-1 and ATF6 dependent) mechanisms during UPR activation [13]. The protein plays a crucial role in the maintenance of calcium homeostasis during ER stress

[14,15]. It has been demonstrated that Herp has an ubiquitin-like domain at the cytoplasmic end, and it is considered to play a role in ERAD by recruiting ubiquitin [16,17]. Herp has also been implicated in the pathogenesis of age-related disorders, including type 2 diabetes [18], neurodegeneration [19–21] and sarcopenia [22]. Herp-deficient neural cells accumulate more amyloid β-protein than wild type cells, and Herp-deficient muscle cells are more susceptible to ER stress-induced apoptosis [21,22]. In spite of these diverse ER stress-associated functions, the role of Herp in the development of atherosclerosis is unknown. We therefore developed a Herp-deficient mouse model of atherosclerosis using apoE deficient mice, and studied whether Herp deficiency affects the development of atherosclerosis.

Materials and Methods

Materials

The anti-Herp antibodies have been described previously [23]. The anti-interleukin-1β (IL-1β), anti-glucose regulated protein 78 kDa (GRP78), normal rabbit IgG (Cell Signaling, Danvers, MA), anti-F4/80 (Abcam, Cambridge, UK) and anti-β-actin (Sigma, St. Louis, MO) antibodies were obtained from commercial sources. Tunicamycin, dimethyl sulfoxide (DMSO) (Sigma), fetal bovine serum (FBS) (HyClone, Logan, UT) and Dulbecco's modified Eagle medium (DMEM) (Nissui, Tokyo, Japan) were also commercially available.

Animals

Herp$^{-/-}$ mice were backcrossed for at least 10 generations with C57BL/6J mice (Japan SLC, Shizuoka, Japan) [23]. ApoE$^{-/-}$ mice on the C57BL/6J background were purchased from The Jackson Laboratory (Bar Harbor, ME). To obtain Herp$^{-/-}$; apoE$^{-/-}$ mice, the crosses were set up as follows. Herp$^{-/-}$ mice were crossed to apoE$^{-/-}$ mice to obtain Herp$^{+/-}$; apoE$^{+/-}$ mice. The Herp$^{+/-}$; apoE$^{+/-}$ mice were intercrossed to produce Herp$^{-/-}$; apoE$^{-/-}$ mice. The mice were maintained on a normal diet after weaning. All procedures were performed in accordance with the guidelines for animal welfare of Tokyo Medical and Dental University, and the protocol was approved by the Animal Welfare Committee of the university.

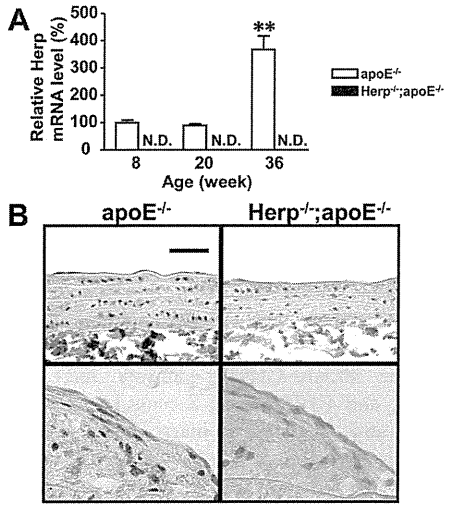

Figure 1. Herp expression in the artery. A: The amount for Herp mRNA was determined by a real-time PCR in the aortas of apoE$^{-/-}$ mice (open columns) and Herp$^{-/-}$; apoE$^{-/-}$mice (closed columns). Each mRNA expression level was normalized to that of GAPDH. The mRNA levels are shown as relative ratios to the mRNA level of eight-week-old apoE$^{-/-}$ mice. Each value represents the mean ± SEM of five mice. N.D. indicates non-detectable. ** $p<0.01$ vs. apoE$^{-/-}$ mice at eight weeks of age. B: Immunostaining of Herp in the normal (upper panels) and atherosclerotic (lower panels) aortas of apoE$^{-/-}$ and Herp$^{-/-}$; apoE$^{-/-}$ mice at 72 weeks of age. Blue; hematoxylin, Red; Herp (diaminobenzidine; DAB). The bar shows 50 μm.
doi:10.1371/journal.pone.0075249.g001

Quantitative analysis of arteriosclerotic lesions and blood chemistry

The atherosclerotic lesions in the aorta were analyzed as described previously [24]. Male apoE$^{-/-}$ and Herp$^{-/-}$; apoE$^{-/-}$ mice were fed a normal diet, and the formation of atherosclerosis was studied at 16, 24, 36 and 72 weeks. After overnight fasting, the mice were anesthetized, a blood sample was drawn from the left ventricle and the entire aorta was resected. The aorta was opened longitudinally from the heart to the femoral arteries, pinned on a wax plate and fixed in 4% paraformaldehyde (Wako, Osaka, Japan). The aorta was photographed with an Olympus C-5050 ZOOM digital camera (Tokyo, Japan). The area of atherosclerotic lesions and the area of the entire aorta was determined using the NIH Image software program. The plasma levels of glucose, cholesterol, triglycerides and non-esterified fatty acid (NEFA) were determined with kits (Wako) as described previously [25].

Histopathology

The aortas were fixed in the 4% paraformaldehyde or snap-frozen in liquid nitrogen. Serial thick sections were stained with hematoxylin-eosin and various antibodies. Briefly, paraffinized sections were deparaffinized, the endogenous peroxidase activity was blocked with 3% H_2O_2 in methanol for 30 min and the samples were stained with an anti-Herp (1:100) antibody using an ABC elite kit (Vector Laboratories, Southfield, MI). Frozen sections were stained with anti-IL-1β (1:100), anti-GRP78 (1:100) or anti-F4/80 (1:1000) antibodies using an ABC elite kit. Unless otherwise indicated, nonspecific immunostaining was not detected in sections stained with normal IgG as the primary antibody or with the secondary antibody alone.

Cell culture

RAW264.7 cells, a mouse macrophage cell line, were obtained from Dainihon-Sumitomo pharmaceutical company (Osaka, Japan), and were cultured in DMEM supplemented with 10% FBS, 50 units/ml penicillin, 50 μg/ml streptomycin and 0.5 μg/ml amphotericin B. Peritoneal macrophages were obtained from eight-week-old apoE$^{-/-}$ or Herp$^{-/-}$; apoE$^{-/-}$ mice. Briefly, 10 ml of sterile PBS were injected into the peritoneal cavity of the mice. The abdomen was gently massaged after its distension. The fluid was recovered and transferred to a sterile tube kept on ice. The cell suspension was centrifuged at 800× g for 5 min at 4°C. The pellet was washed once with chilled PBS and suspended in a volume of RPMI-1640 medium containing 10% FBS, 2 mM glutamine, 50 units/ml penicillin, 50 μg/ml streptomycin and 0.5 μg/ml amphotericin B. Cells were plated and incubated for 2 h at 37°C in a humidified CO_2 (5%) incubator. The monolayers were washed with PBS three times to remove non-adherent cells, and monolayers were incubated overnight at 37°C in the above RPMI medium before being studied.

ER stress was induced by treatment with 1–10 μM tunicamycin (Sigma). The cell viability was measured by the 4-[3-(4-Iodophenyl)-2-(4-nitrophenyl)-2H-5-tetrazolio]-1, 3- benzene disulfonate (WST-1) assay (Roche Diagnostics, Basel, Switzerland).

Immunoblotting

The immunoblot analysis of Herp in the aorta was conducted as reported previously [26]. The aorta was homogenized in ice-cold homogenization buffer (50 mM Tris-HCl, pH 8.0, 150 mM NaCl, 1% Triton-X100 and 1% protease inhibitor cocktail [Sigma]) with a physcotron NS-310E homogenizer (Microtec, Chiba, Japan). Proteins (10 μg) were run under reducing conditions on 5–20% gradient polyacrylamide gels and were transferred to PVDF membranes. The membrane was blocked in blocking buffer (5% fish gelatin and 0.5% Tween-20 in TBS) for 1 h, and then incubated with anti-Herp (1:500) or anti-β-actin (1:1000) antibodies in blocking buffer overnight at 4°C. After being washed with 0.5% Tween-20 in TBS, the membrane was incubated for 2 h with a HRP-conjugated secondary antibody and visualized using the ECL plus Western Blotting Detection System (GE Healthcare, Fairfield, CT).

Transfection

Transfections of siRNA were performed with Lipofectamine 2000 (Invitrogen, Carlsbad, CA) as directed by the manufacturer. Briefly, cells were seeded at 2×10^5 per well in six-well plates, then on the following day were transfected with 5 μl of Lipofectamine 2000 combined with 200 pmol of siRNA. The transfection mixtures were left on cells for 4 h, and then replaced with fresh media. At 48 h post-transfection, the cells were treated with tunicamycin (10 μM) or DMSO for 6 h. The siRNA against mouse Herp (sense sequence: 5′-UGG AUC ACC AGU GUC UCC AAG AUU U-3′, antisense sequence: 5′-AAA UCU UGG AGA CAC UGG UGA UCC A-3′) and negative control siRNA were obtained from Invitrogen.

Real-time PCR analysis

Total RNA was prepared from each aorta using the RNeasy Mini kit (Qiagen, Duesseldorf, Germany). The first-strand cDNA was synthesized from 1 μg of total RNA using Omniscript Reverse Transcription (Qiagen). The real-time RT-PCR analyses were performed as described previously [27] using 10 ng of cDNA and TaqMan probes (Roche Diagnostics) for IL-1β, interleukin-6 (IL-6), monocyte chemoattractant protein-1 (MCP-1), stress-associated endoplasmic reticulum protein 1 (SERP1), Sec61b, sel-1 homolog 1 (SEL1L) and activating transcription factor 4 (ATF4) with a LightCycler instrument (Roche Diagnostics). The mRNA expression levels of Herp, GRP78, C/EBP homologous protein (CHOP), tumor necrosis factor-α (TNF-α, vascular cell adhesion molecule (VCAM) and glyceraldehyde-3- phosphate dehydrogenase (GAPDH), were evaluated as described previously with SYBR Green (Roche Diagnostics) [27]. The amount of target mRNA was normalized to that of GAPDH in the same sample. The RT-PCR for XBP1 was designed to amplify both the 140 bp (unspliced form) and 114 bp (spliced form) products [23]. The primers used for real-time PCR are listed in Table S1.

Statistical analysis

The data were compared with a one-way ANOVA, followed by Scheffe's multiple comparison test or Student's *t* test. A value of $P<0.05$ was considered to be statistically significant. All values are expressed as the means ± SEM.

Results

Herp is expressed in the normal arteries

To assess the role of Herp in the arteries, we first evaluated the expression levels of Herp in the arteries. Herp mRNA was detected in the aortas of apoE$^{-/-}$ mice, but not in Herp$^{-/-}$; apoE$^{-/-}$ mice (Fig. 1A). The Herp mRNA expression was significantly increased in the older (36 weeks) mice (Fig. 1A). Immunostaining revealed that Herp was mainly expressed in smooth muscle cells. However, Herp was not detected in the endothelial cells in normal aorta (Fig. 1B). In atherosclerotic lesions, Herp was expressed in a portion of the macrophages (not in all macrophages), endothelial cells and smooth muscle cells (Fig. 1B, Fig. S1).

The deficiency of Herp suppresses the development of atherosclerosis in apoE$^{-/-}$ mice

Next, we examined the effects of Herp on the development of atherosclerosis. The deficiency of Herp significantly suppressed the development of atherosclerosis in apoE$^{-/-}$ mice (Figs. 2A, B). At 16 weeks, the apoE$^{-/-}$ mice developed small fatty streaks at the aortic arch, whereas Herp$^{-/-}$; apoE$^{-/-}$ mice did not develop these lesions. At 24 weeks, the apoE$^{-/-}$ mice developed sizable lesions at the arch, while Herp$^{-/-}$; apoE$^{-/-}$ mice had less developed lesions at the arch than apoE$^{-/-}$ mice. At 36 weeks, the apoE$^{-/-}$ mice had lesions in both the arch and abdominal aorta, while Herp$^{-/-}$; apoE$^{-/-}$ mice had atherosclerotic lesions only in the arch. At 72 weeks, the apoE$^{-/-}$ mice showed atherosclerotic lesions that covered almost 50% of the entire aortic surface. In contrast, the Herp$^{-/-}$; apoE$^{-/-}$ mice had lesions that covered less than 30% of the surface (Figs. 2A, B).

Herp deficiency affects the plasma glucose and lipid levels

The development of atherosclerosis is driven by high plasma levels of cholesterol [28,29]. Since the response to ER stress results in lipogenic and cholesterogenic gene expression in hepatocytes [30], it is possible that Herp-deficiency affected the lesion formation by changing the plasma levels of lipids. We therefore determined the plasma levels of cholesterol, triglycerides and NEFA. The body weights were not significantly different between the apoE$^{-/-}$ and Herp$^{-/-}$;apoE$^{-/-}$ mice (Fig. 3A). However, the levels of glucose were significantly higher in Herp$^{-/-}$;apoE$^{-/-}$

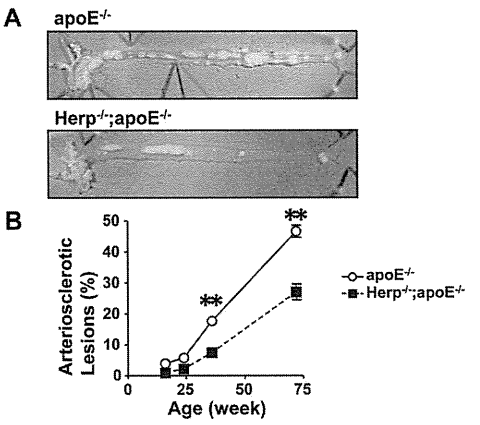

Figure 2. Herp deficiency suppressed the development of atherosclerosis in apoE$^{-/-}$ mice. A: Photographs of the aortas of apoE$^{-/-}$ (upper panel) and Herp$^{-/-}$; apoE$^{-/-}$ (lower panel) mice at 72 weeks of age. The aorta was opened longitudinally from the heart to the femoral arteries. The white plaques are atherosclerotic lesions. B: A quantitative analysis of the atherosclerotic lesions. The area was determined using the NIH Image software program. Each point represents the percentage of the lesion to the entire aorta. Open circles show apoE$^{-/-}$, and closed squares show Herp$^{-/-}$; apoE$^{-/-}$ mice. Each value represents the mean ± SEM of four to six mice. ** $p<0.01$ vs. Herp$^{-/-}$; apoE$^{-/-}$ mice at the same age.
doi:10.1371/journal.pone.0075249.g002

$^{-}$ than in apoE$^{-/-}$ mice at eight, 16, 24 and 36 weeks (Fig. 3B). There were no significant differences in the plasma levels of cholesterol and triglycerides between the Herp$^{-/-}$; apoE$^{-/-}$ and apoE$^{-/-}$ mice (Figs. 3C, D). The plasma NEFA level was higher in apoE$^{-/-}$ than Herp$^{-/-}$; apoE$^{-/-}$ mice at eight and 16 weeks, but not thereafter (Fig. 3E).

Herp-deficiency attenuates the ER stress-induced unfolded protein response (UPR) and inflammation in the aorta

Activation of the UPR is observed at all stages of atherosclerotic lesion development in apoE$^{-/-}$ mice [1]. We therefore assessed the UPR in the aortas of Herp-deficient mice. The amount of mRNA for inflammatory cytokines, such as IL-1β, IL-6 and MCP-1, was significantly lower in Herp$^{-/-}$; apoE$^{-/-}$ mice than in apoE$^{-/-}$ mice (Figs. 4A, C, D). Among the various ER stress-related proteins, we found that the amount of mRNA for GRP78 was significantly lower in Herp$^{-/-}$; apoE$^{-/-}$ mice than in apoE$^{-/-}$ mice (Fig. 4B), while that for CHOP showed a slight, but statistically significant, decrease in the Herp$^{-/-}$; apoE$^{-/-}$ mice (Fig. 4E). The amount of mRNA for VCAM-1 was also lower in Herp$^{-/-}$; apoE$^{-/-}$ mice (Fig. 4F). We also examined the expression of factors involved in other ER stress pathways, including IRE1, PERK and ATF6. The amount of mRNA for stress-associated endoplasmic reticulum protein 1 (SERP1) and Sec61b, an IRE1/XBP-1-dependent gene, was significantly decreased at 20 weeks in Herp$^{-/-}$; apoE$^{-/-}$ mice (Figs. 4G, H). The amount of mRNA for sel-1 homolog 1 (SEL1L) (Fig. 4I) and protein disulfide isomerase family A member 4 (PDIA4) (data not shown), ATF6-dependent genes, was not significantly different between apoE$^{-/-}$ and Herp$^{-/-}$; apoE$^{-/-}$ mice (Fig. 4I). The amount of mRNA for activating transcription factor 4 (ATF4), a PERK-dependent gene, was significantly different at 20 and 32 weeks in Herp$^{-/-}$; apoE$^{-/-}$ mice (Fig. 4J) compared to the apoE$^{-/-}$ mice.

An immunohistological analysis of the atherosclerotic lesions confirmed the results of the above-mentioned mRNA analyses. The IL-1β expression in macrophages was suppressed in atherosclerotic lesions of the Herp$^{-/-}$; apoE$^{-/-}$ mice (Fig. 4A). Consistent with previous reports [1,31], GRP78 was extensively expressed in macrophage-derived foam cells of atherosclerotic lesions. The expression of the GRP78 protein was lower in Herp$^{-/-}$; apoE$^{-/-}$ mice (Fig. 4B).

Herp-deficiency attenuates the tunicamycin-induced UPR and inflammatory responses in macrophages

An immunohistological study suggested that Herp-deficiency suppressed the ER stress responses, particularly in the macrophages in atherosclerotic lesions. We therefore studied the effects of Herp-deficiency in macrophages *in vitro*.

Consistent with previous reports [9,32], inflammatory cytokines, such as IL-1β, IL-6, TNF-α and MCP-1, were induced in the macrophages of apoE$^{-/-}$ mice. The induction of these cytokines was decreased in the macrophages from Herp$^{-/-}$; apoE$^{-/-}$ mice (Figs. 5A, B, F, G). The amount of mRNA for SERP1 and Sec61b was significantly decreased in tunicamycin-treated macrophages from Herp$^{-/-}$; apoE$^{-/-}$ mice compared to apoE$^{-/-}$ mice (Figs. 5H, I). The amount of mRNA for SEL1L was not significantly different between apoE$^{-/-}$ and Herp$^{-/-}$; apoE$^{-/-}$ mice (Fig. 5J). The amount of mRNA for ATF4 was significantly attenuated in tunicamycin-treated macrophages from Herp$^{-/-}$; apoE$^{-/-}$ mice compared with apoE$^{-/-}$ mice (Fig. 5K).

Cultured peritoneal macrophages minimally expressed ER stress-related proteins, GRP78, CHOP and Herp, when they were unstimulated. However, once they were stimulated with tunicamycin, the peritoneal macrophages from apoE$^{-/-}$ mice expressed GRP78, CHOP and Herp. In contrast, the peritoneal

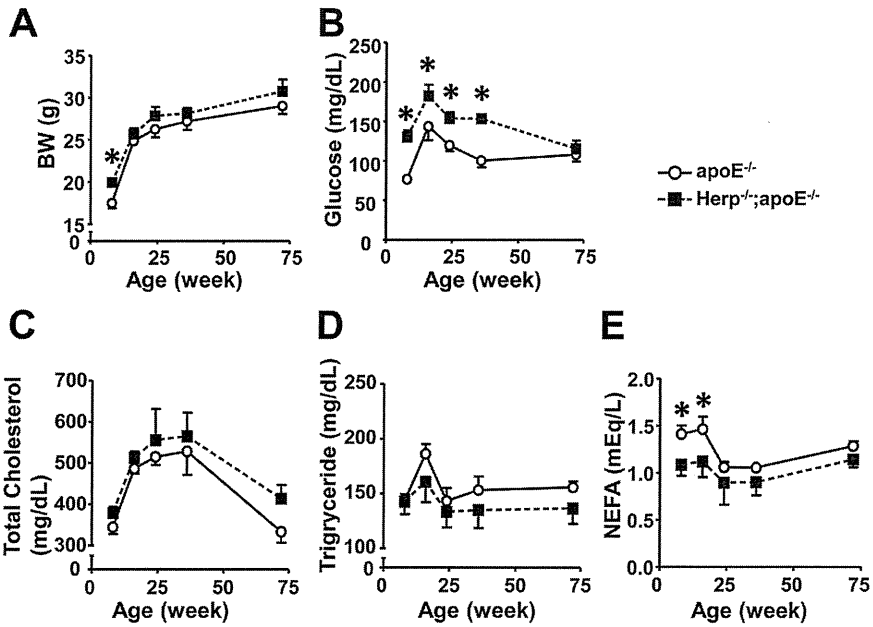

Figure 3. Effect of Herp deficiency on the plasma glucose and lipid levels. The body weight (A) and the plasma levels of glucose (B), cholesterol (C), triglycerides (D) and NEFA (E) following overnight fasting at eight, 16, 24, 36 and 72 weeks of age, were determined as described in the Methods. Open circles show apoE$^{-/-}$, and closed squares show Herp$^{-/-}$; apoE$^{-/-}$ mice. Each value represents the mean ± SEM; n = 5 per group. * $p<0.01$ vs. Herp$^{-/-}$; apoE$^{-/-}$ mice at the same age.
doi:10.1371/journal.pone.0075249.g003

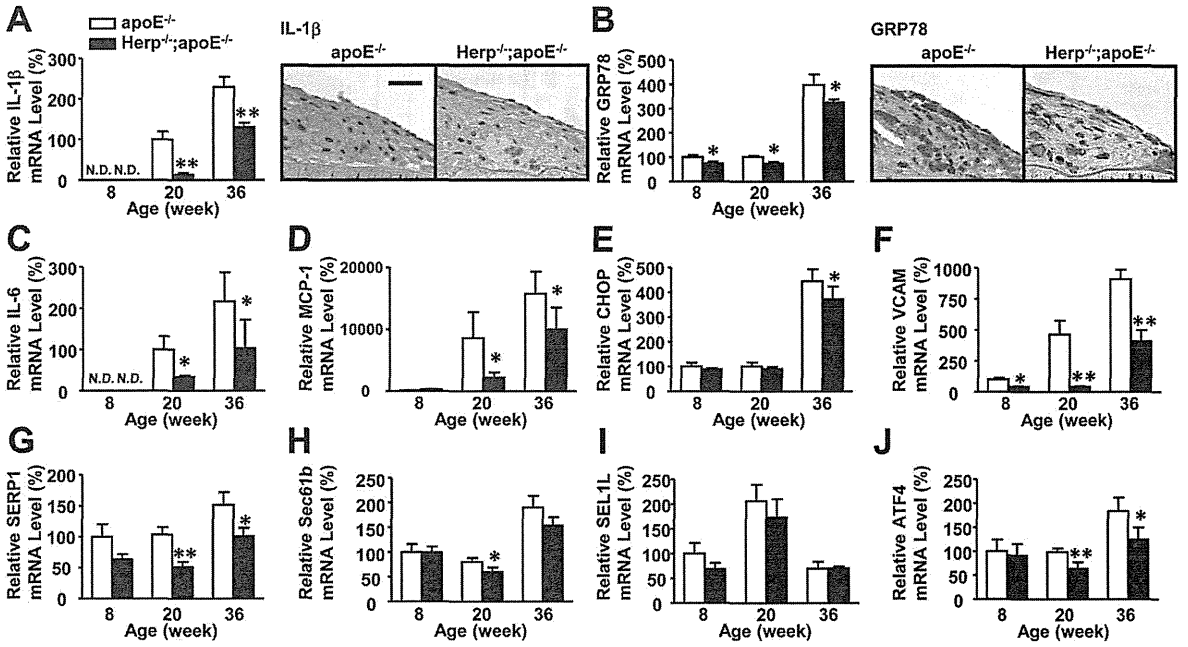

Figure 4. The expression levels of IL-1β, MCP-1 and VCAM-1 were reduced in the aortas of Herp$^{-/-}$; apoE$^{-/-}$ mice. Total RNA was prepared from the entire aortas of apoE$^{-/-}$ and Herp$^{-/-}$; apoE$^{-/-}$ mice. The mRNA expression levels were determined by real-time PCR. Each mRNA level was normalized to that of GAPDH mRNA. The mRNA levels are shown as the relative ratio to the mRNA level of eight or 20-week-old apoE$^{-/-}$ mice. A: IL-1β, B: GRP78, C: IL-6, D: MCP-1, E: CHOP, F: VCAM-1, G: SERP1, H: Sec61b, I: SEL1L and J: ATF4. Open columns show apoE$^{-/-}$, and closed columns show Herp$^{-/-}$; apoE$^{-/-}$ mice. Each column represents the mean ± SEM of five mice. N.D. indicates non-detectable. * $p<0.05$, ** $p<0.01$ vs. apoE$^{-/-}$ mice at the same age. A, B: Immunostaining of IL-1β and GRP78 in the atherosclerotic aortas of apoE$^{-/-}$ and Herp$^{-/-}$; apoE$^{-/-}$ mice at 72 weeks of age. Blue; hematoxylin, Red; GRP78 or IL-1β (DAB). The bar shows 50 μm.
doi:10.1371/journal.pone.0075249.g004

macrophages from Herp$^{-/-}$; apoE$^{-/-}$ mice expressed significantly less GRP78 and CHOP, and did not express Herp at all (Figs. 5C, D, E).

The role of Herp in the ER stress response was further confirmed by treating RAW264.7 macrophages with a siRNA against Herp. Tunicamycin treatment induced the expression of ER stress response genes (such as GRP78 and CHOP) and Herp, and inflammation-related genes (such as IL-1β and IL-6) (Figs. 6A–E). The siRNA against Herp decreased the amount of Herp mRNA by 90% in RAW264.7 macrophages treated with tunicamycin, while the control siRNA did not affect the amount of Herp mRNA (Fig. 6C). Of note, the induction of GRP78, CHOP, IL-1β, IL-6, SERP1 and Sec61b was significantly suppressed by the treatment of the cells with the siRNA against Herp (Figs. 6A, B, D, E, H, I). However, there were no significant differences between control and siHerp-treated cells in terms of the ER stress-induced ATF4 mRNA expression (Fig. 6K). The mRNA levels of MCP-1 and TNF-α were decreased by tunicamycin treatment (Figs. 6F, G).

The mRNA expression of IRE1 dependent genes, such as SERP1 and Sec61b, was suppressed by Herp deficiency in macrophages from apoE$^{-/-}$ and Herp$^{-/-}$;apoE$^{-/-}$ mice (Fig. 4) and RAW264.7 cells (Fig. 5). However, XBP-1 splicing was not prevented by Herp deficiency in macrophages and RAW264.7 cells (Fig. S2).

ER stress induces apoptosis in macrophages, which may suppress the development of atherosclerosis [33]. Tunicamycin caused a similar level of apoptosis in the peritoneal macrophages from both Herp$^{-/-}$; apoE$^{-/-}$ and apoE$^{-/-}$ mice (Fig. S3).

Discussion

A major novel finding of this study is that Herp deficiency suppressed the ER stress-induced inflammation and attenuated the development of atherosclerosis without affecting the plasma levels of cholesterol or triglyceride. Our findings indicate that Herp is also an essential component of ER stress-induced inflammation.

The precise mechanisms underlying the suppression of inflammatory cytokine production due to Herp deficiency are unclear. However, there are several possible mechanisms based on the functions of Herp that have been previously reported by others. First, recent reports have shown that these inflammatory cytokines are regulated by ER stress, primarily via the CHOP pathway [9,34,35]. CHOP deficiency also decreases the expression of inflammatory cytokines in arteries and suppresses arteriosclerosis in apoE-deficient mice [9]. Similar to CHOP deficiency, Herp deficiency suppresses ER stress-induced inflammation and attenuates the development of atherosclerosis. Our study showed that Herp deficiency decreases the expression of CHOP in the aortas. Herp may therefore regulate ER stress-induced inflammation by decreasing the CHOP expression. However, the effects of Herp deficiency cannot be attributed solely to a decrease in the CHOP expression [8] because CHOP deficiency, not Herp deficiency, decreases apoptosis among macrophages (Fig. S3). Herp deficiency might be more efficient for reducing the inflammatory response than for inducing the apoptosis of macrophages. Second, the suppression of IL-1β and TNF-α by Herp deficiency may involve the PERK – NF-κB pathway. The mRNA expression levels of molecules downstream of the PERK pathway, such as ATF4, were significantly attenuated by a Herp deficiency in the aorta and the tunicamycin-treated macrophages. The attenuated PERK-medi-

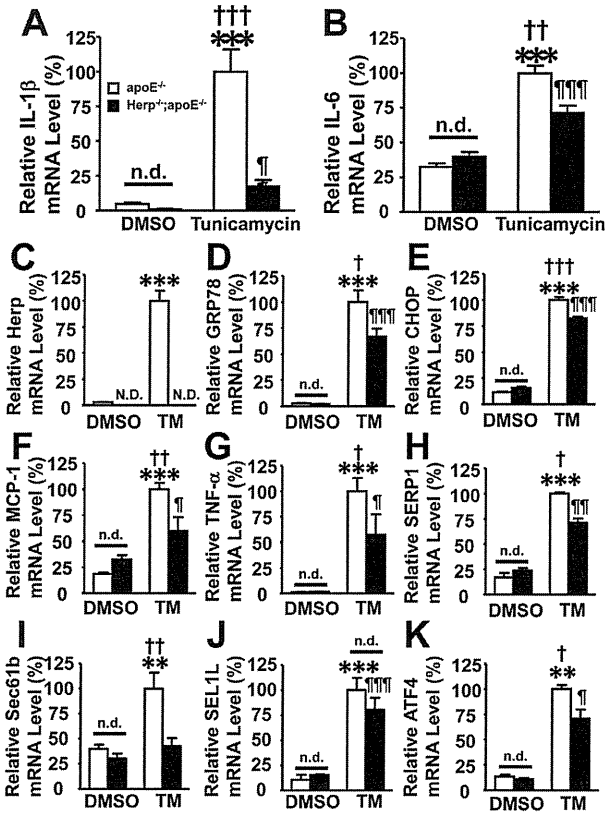

Figure 5. Herp-deficient peritoneal macrophages showed reduced expression of IL-1β and IL-6 in response to ER stress. Peritoneal macrophages were prepared from eight-week-old apoE$^{-/-}$ and Herp$^{-/-}$; apoE$^{-/-}$ mice, and were stimulated with 10 μM tunicamycin for 6 hrs. The mRNA levels of ER stress-related proteins and cytokines were analyzed by a real-time PCR analysis. Open columns show unstimulated cells (DMSO), and closed columns show cells stimulated with tunicamycin (TM). Each amount of mRNA was normalized to GAPDH. The mRNA levels are shown as the relative ratio to the mRNA level of tunicamycin-treated macrophages from apoE$^{-/-}$ mice. A: IL-1β, B: IL-6, C: Herp, D: GRP78, E: CHOP, F: MCP-1, G: TNF-α, H: SERP1, I: Sec61b, J: SEL1L and K: ATF4. Each column represents the mean ± SEM; n = 5 per group. ** $p<0.01$, *** $p<0.001$, vs unstimulated apoE$^{-/-}$ macrophages; ¶$p<0.05$, ¶¶$p<0.01$, ¶¶¶$p<0.001$ vs unstimulated Herp$^{-/-}$; apoE$^{-/-}$ peritoneal macrophages. †$p<0.05$, ††$p<0.01$, †††$p<0.001$ vs stimulated Herp$^{-/-}$; apoE$^{-/-}$ peritoneal macrophages. N.D.; not detected. n.d.; no difference.
doi:10.1371/journal.pone.0075249.g005

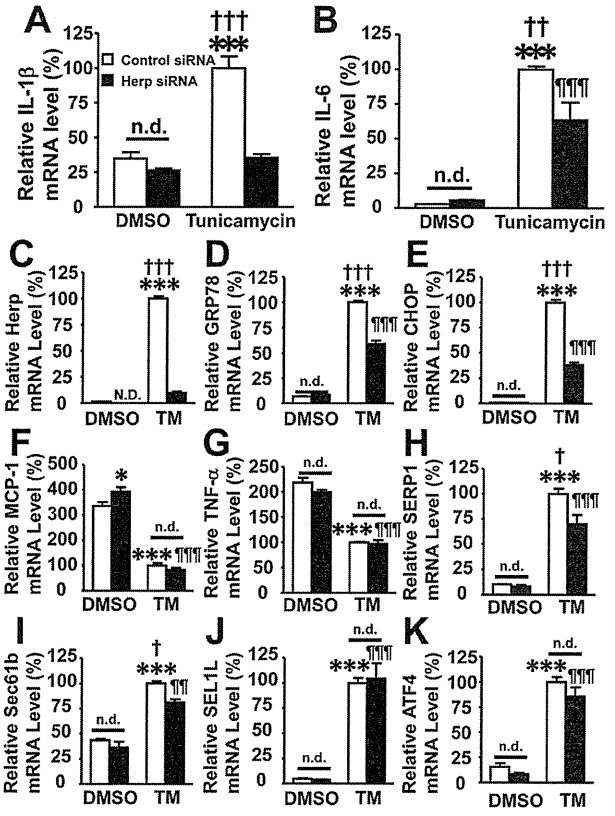

Figure 6. Herp-deficient RAW264.7 macrophages showed reduced expression of IL-1β and IL-6 in response to ER stress. RAW264.7 macrophages were treated with a siRNA against Herp or a control siRNA for 48 hrs, and then ER stress was induced with 10 μM tunicamycin for 6 hrs. The mRNA expression levels of ER stress-related proteins and cytokines were analyzed by a real-time PCR analysis. Open columns show unstimulated cells (DMSO), closed columns show cells stimulated with tunicamycin (TM). The amounts of mRNA were normalized to that of GAPDH. The mRNA levels were shown as a relative ratio to the mRNA level of tunicamycin-treated macrophages, which were transfected with control siRNA. A: IL-1β, B: IL-6, C: Herp, D: GRP78, E: CHOP, F: MCP-1, G: TNF-α, H: SERP1, I: Sec61b, J: SEL1L and K: ATF4. Each column represents the mean ± SEM; n = 3 per group. * $p<0.05$, ** $p<0.01$, *** $p<0.001$, vs unstimulated control macrophages; ¶$p<0.05$, ¶¶$p<0.01$, ¶¶¶$p<0.001$ vs unstimulated siHerp macrophages. †$p<0.05$, ††$p<0.01$, †††$p<0.001$ vs stimulated siHerp macrophages. N.D.; not detected. n.d.; no difference.
doi:10.1371/journal.pone.0075249.g006

ated reduction in the level of IκB results in a decreased NF-κB activation [36]. In contrast to ATF4, ATF6, another molecule that regulates NF-κB activation upon ER stress [10,11], is not involved in the decrease in the mRNA expression of IL-1β and TNF-α in Herp-deficient mice. In this study, we showed that Herp deficiency does not affect the mRNA expression of SEL1L (Figs. 4I, 5J, 6J) or PID1A (data not shown), which are ATF6-dependent genes. Finally, the decrease in NEFA due to Herp deficiency may contribute to the suppression of inflammation in apoE-deficient mice. A deficiency of Herp caused a transient mild decrease in the plasma NEFA concentration at eight and 16 weeks in these mice (Fig. 3C). Since NEFA induces ER stress and inflammation, the decrease in NEFA may explain the attenuation of atherosclerosis in the Herp$^{-/-}$;apoE$^{-/-}$ mice. However, the lower level of NEFA may not be the major reason for the reduction in ER stress-induced inflammatory reactions because the change in the NEFA concentrations was mild, and a reduction in the inflammation-related gene expression due to Herp deficiency was observed in both the Herp-deleted peritoneal macrophages and RAW264.7 cells *in vitro*. Why the concentrations of NEFA were lower in the Herp$^{-/-}$;apoE$^{-/-}$ mice is not clear. A possible explanation is a reduction in the ER stress response in the adipose tissue. ER stress in adipocytes induces lipolysis by activating the cAMP/PKA and ERK1/2 pathways [37]. If the reduction of the ER stress response occurred in the adipose tissue of Herp$^{-/-}$;apoE$^{-/-}$ mice, the plasma levels of NEFA may be lower in Herp$^{-/-}$;apoE$^{-/-}$ mice than in apoE$^{-/-}$ mice.

The induction of MCP-1 and TNF-α mRNA was attenuated by tunicamycin treatment in the macrophages collected from the Herp$^{-/-}$; apoE$^{-/-}$ mice (Figures 5F, G). However, the tunicamycin-treated RAW264.7 cells exhibited a decreased mRNA expression of MCP-1 and TNF-α, regardless of the presence or absence of Herp (Figure 6). These reductions were not

observed in the RAW 264.7 cells possibly because the RAW264.7 cells were established by the inoculum of the moloney murine leukemia virus (MuLV) [38]. RAW264.7 cells also express polytropic MuLV [39], which may not possess functional p53 [40]. We therefore considered that these differences between the primary cultured macrophages and RAW264.7 cells were caused by the differences in the degree of activated p53. However, further studies are required to investigate these mechanisms.

We also showed that Herp has a unique expression pattern, wherein it is expressed not only in a small portion of macrophages in atherosclerotic lesions, but also smooth muscle cells (SMCs) in normal aorta (Fig. 1B). Of note, the expression levels of Herp are not upregulated at 20 weeks in apoE$^{-/-}$ mice (Fig. 1A). The expression of Herp was not increased in the media that underlie the atherosclerotic plaques. In contrast, GRP78 was vigorously expressed in most macrophages in the lesions and increased in the lesions underlying the atherosclerotic plaques (Fig. 4G) [1,31]. There are two major roles of Herp that have been speculated based on previous reports in other tissues. These include the secretion of proteins [41] and calcium homeostasis [2]. Herp plays a role in the ER stress response, likely due to the production of extracellular matrix proteins. And Herp may be expressed in the SMCs of normal aortas because it stabilizes the Ca^{2+} storage in the ER.

In summary, we herein reported a novel function of Herp in ER stress-induced inflammation, and described its potential role in the development of atherosclerosis.

Supporting Information

Figure S1 Herp was expressed in a subset of macrophages and smooth muscle cells in atherosclerotic lesions. Immunostaining of the aorta from apoE$^{-/-}$ mice. Blue; hematoxylin, Red; Herp (diaminobenzidine; DAB). The bar shows 50 μm.
(TIF)

Figure S2 Herp deficiency did not increase the XBP-1 splicing in macrophages. Peritoneal macrophages were prepared from apoE$^{-/-}$ and Herp$^{-/-}$; apoE$^{-/-}$ mice, and stimulated with 1 to 10 μM tunicamycin for 6 hrs. The transfection of siHerp into RAW264.7 cells was described in the Methods section. RT-PCR for XBP1 was designed to amplify both the 140 bp (unspliced form) and 114 bp (spliced form) products.
(TIF)

Figure S3 Herp deficiency did not increase the ER stress-induced apoptosis in macrophages. Peritoneal macrophages were prepared from apoE$^{-/-}$ and Herp$^{-/-}$; apoE$^{-/-}$ mice, and were stimulated with 1 to 10 μM tunicamycin for 6 hrs. The cell viability was determined as described in the Methods.
(TIF)

Table S1 Real-time PCR and PCR primers. The real-time PCR primers were designed to anneal to the indicated sequences using the free Primer3 software program (http://frodo.wi.mit.edu/cgi-bin/primer3/primer3_www.cgi).
(DOC)

Acknowledgments

We are grateful to Dr. Masayuki Yoshida for valuable discussions. We also thank Kaoru Hatori and Hiroki Ueda for their expert technical assistance.

Author Contributions

Conceived and designed the experiments: SS TC EK KS. Performed the experiments: SS TC KK. Analyzed the data: SS TC KK KS. Contributed reagents/materials/analysis tools: EK KK TM. Wrote the paper: SS KS.

References

1. Zhou J, Lhotak S, Hilditch BA, Austin RC (2005) Activation of the unfolded protein response occurs at all stages of atherosclerotic lesion development in apolipoprotein E-deficient mice. Circulation 111: 1814–1821.
2. Scull CM, Tabas I (2011) Mechanisms of ER stress-induced apoptosis in atherosclerosis. Arterioscler Thromb Vasc Biol 31: 2792–2797.
3. Tabas I (2010) The role of endoplasmic reticulum stress in the progression of atherosclerosis. Circ Res 107: 839–850.
4. Anderson EK, Hill AA, Hasty AH (2012) Stearic acid accumulation in macrophages induces toll-like receptor 4/2-independent inflammation leading to endoplasmic reticulum stress-mediated apoptosis. Arterioscler Thromb Vasc Biol 32: 1687–1695.
5. Devries-Seimon T, Li Y, Yao PM, Stone E, Wang Y, et al. (2005) Cholesterol-induced macrophage apoptosis requires ER stress pathways and engagement of the type A scavenger receptor. J Cell Biol 171: 61–73.
6. Minamino T, Komuro I, Kitakaze M (2010) Endoplasmic reticulum stress as a therapeutic target in cardiovascular disease. Circ Res 107: 1071–1082.
7. Arai S, Shelton JM, Chen M, Bradley MN, Castrillo A, et al. (2005) A role for the apoptosis inhibitory factor AIM/Spalpha/Api6 in atherosclerosis development. Cell Metab 1: 201–213.
8. Thorp E, Li G, Seimon TA, Kuriakose G, Ron D, et al. (2009) Reduced apoptosis and plaque necrosis in advanced atherosclerotic lesions of Apoe−/− and Ldlr−/− mice lacking CHOP. Cell Metab 9: 474–481.
9. Gao J, Ishigaki Y, Yamada T, Kondo K, Yamaguchi S, et al. (2011) Involvement of endoplasmic stress protein C/EBP homologous protein in arteriosclerosis acceleration with augmented biological stress responses. Circulation 124: 830–839.
10. Yamazaki H, Hiramatsu N, Hayakawa K, Tagawa Y, Okamura M, et al. (2009) Activation of the Akt-NF-kappaB pathway by subtilase cytotoxin through the ATF6 branch of the unfolded protein response. J Immunol 183: 1480–1487.
11. Zhang K, Shen X, Wu J, Sakaki K, Saunders T, et al. (2006) Endoplasmic reticulum stress activates cleavage of CREBH to induce a systemic inflammatory response. Cell 124: 587–599.
12. Kokame K, Agarwala KL, Kato H, Miyata T (2000) Herp, a new ubiquitin-like membrane protein induced by endoplasmic reticulum stress. J Biol Chem 275: 32846–32853.
13. Ma Y, Hendershot LM (2004) Herp is dually regulated by both the endoplasmic reticulum stress-specific branch of the unfolded protein response and a branch that is shared with other cellular stress pathways. J Biol Chem 279: 13792–13799.
14. Chan SL, Fu W, Zhang P, Cheng A, Lee J, et al. (2004) Herp stabilizes neuronal Ca2+ homeostasis and mitochondrial function during endoplasmic reticulum stress. J Biol Chem 279: 28733–28743.
15. Tuvia S, Taglicht D, Erez O, Alroy I, Alchanati I, et al. (2007) The ubiquitin E3 ligase POSH regulates calcium homeostasis through spatial control of Herp. J Cell Biol 177: 51–61.
16. Schulze A, Standera S, Buerger E, Kikkert M, van Voorden S, et al. (2005) The ubiquitin-domain protein HERP forms a complex with components of the endoplasmic reticulum associated degradation pathway. J Mol Biol 354: 1021–1027.
17. Lilley BN, Ploegh HL (2004) A membrane protein required for dislocation of misfolded proteins from the ER. Nature 429: 834–840.
18. Yan S, Zheng C, Chen ZQ, Liu R, Li GG, et al. (2012) Expression of endoplasmic reticulum stress-related factors in the retinas of diabetic rats. Exp Diabetes Res 2012: 743780.
19. Chigurupati S, Wei Z, Belal C, Vandermey M, Kyriazis G, et al. (2009) The homocysteine-inducible endoplasmic reticulum stress protein counteracts calcium store depletion and induction of C/EBP homologous protein in a neurotoxin model of Parkinson's disease. J Biol Chem.
20. Slodzinski H, Moran LB, Michael GJ, Wang B, Novoselov S, et al. (2009) Homocysteine-induced endoplasmic reticulum protein (herp) is up-regulated in parkinsonian substantia nigra and present in the core of Lewy bodies. Clin Neuropathol 28: 333–343.
21. Sai X, Kokame K, Shiraishi H, Kawamura Y, Miyata T, et al. (2003) The ubiquitin-like domain of Herp is involved in Herp degradation, but not necessary for its enhancement of amyloid beta-protein generation. FEBS Lett 553: 151–156.
22. Nogalska A, Engel WK, McFerrin J, Kokame K, Komano H, et al. (2006) Homocysteine-induced endoplasmic reticulum protein (Herp) is up-regulated in sporadic inclusion-body myositis and in endoplasmic reticulum stress-induced cultured human muscle fibers. J Neurochem 96: 1491–1499.

23. Eura Y, Yanamoto H, Arai Y, Okuda T, Miyata T, et al. (2012) Derlin-1 deficiency is embryonic lethal, Derlin-3 deficiency appears normal, and Herp deficiency is intolerant to glucose load and ischemia in mice. PLoS One 7: e34298.
24. Chiba T, Kondo Y, Shinozaki S, Kaneko E, Ishigami A, et al. (2006) A selective NFkappaB inhibitor, DHMEQ, reduced atherosclerosis in ApoE-deficient mice. J Atheroscler Thromb 13: 308–313.
25. Chiba T, Shinozaki S, Nakazawa T, Kawakami A, Ai M, et al. (2007) Leptin deficiency suppresses progression of atherosclerosis in apoE-deficient mice. Atherosclerosis.
26. Higaki M, Shimokado K (1999) Phosphatidylinositol 3-kinase is required for growth factor-induced amino acid uptake by vascular smooth muscle cells. Arterioscler Thromb Vasc Biol 19: 2127–2132.
27. Shinozaki S, Chiba T, Kokame K, Miyata T, Ai M, et al. (2007) Site-specific effect of estradiol on gene expression in the adipose tissue of ob/ob mice. Horm Metab Res 39: 192–196.
28. Ross R (1999) Atherosclerosis is an inflammatory disease. Am Heart J 138: S419–420.
29. Meir KS, Leitersdorf E (2004) Atherosclerosis in the apolipoprotein-E-deficient mouse: a decade of progress. Arterioscler Thromb Vasc Biol 24: 1006–1014.
30. Parker RA, Flint OP, Mulvey R, Elosua C, Wang F, et al. (2005) Endoplasmic reticulum stress links dyslipidemia to inhibition of proteasome activity and glucose transport by HIV protease inhibitors. Mol Pharmacol 67: 1909–1919.
31. Zhou J, Werstuck GH, Lhotak S, de Koning AB, Sood SK, et al. (2004) Association of multiple cellular stress pathways with accelerated atherosclerosis in hyperhomocysteinemic apolipoprotein E-deficient mice. Circulation 110: 207–213.
32. Zhou AX, Tabas I (2013) The UPR in atherosclerosis. Semin Immunopathol 35: 321–332.
33. Liu J, Thewke DP, Su YR, Linton MF, Fazio S, et al. (2005) Reduced macrophage apoptosis is associated with accelerated atherosclerosis in low-density lipoprotein receptor-null mice. Arterioscler Thromb Vasc Biol 25: 174–179.
34. Endo M, Mori M, Akira S, Gotoh T (2006) C/EBP homologous protein (CHOP) is crucial for the induction of caspase-11 and the pathogenesis of lipopolysaccharide-induced inflammation. J Immunol 176: 6245–6253.
35. Suyama K, Ohmuraya M, Hirota M, Ozaki N, Ida S, et al. (2008) C/EBP homologous protein is crucial for the acceleration of experimental pancreatitis. Biochem Biophys Res Commun 367: 176–182.
36. Hotamisligil GS (2010) Endoplasmic reticulum stress and the inflammatory basis of metabolic disease. Cell 140: 900–917.
37. Deng J, Liu S, Zou L, Xu C, Geng B, et al. (2012) Lipolysis response to endoplasmic reticulum stress in adipose cells. J Biol Chem 287: 6240–6249.
38. Raschke WC, Baird S, Ralph P, Nakoinz I (1978) Functional macrophage cell lines transformed by Abelson leukemia virus. Cell 15: 261–267.
39. Hartley JW, Evans LH, Green KY, Naghashfar Z, Macias AR, et al. (2008) Expression of infectious murine leukemia viruses by RAW264.7 cells, a potential complication for studies with a widely used mouse macrophage cell line. Retrovirology 5: 1.
40. Wong KS, Li YJ, Howard J, Ben-David Y (1999) Loss of p53 in F-MuLV induced-erythroleukemias accelerates the acquisition of mutational events that confers immortality and growth factor independence. Oncogene 18: 5525–5534.
41. Hartley T, Siva M, Lai E, Teodoro T, Zhang L, et al. (2010) Endoplasmic reticulum stress response in an INS-1 pancreatic beta-cell line with inducible expression of a folding-deficient proinsulin. BMC Cell Biol 11: 59.

Molecular Cell
Article

Autoadaptive ER-Associated Degradation Defines a Preemptive Unfolded Protein Response Pathway

Riccardo Bernasconi,[1] Carmela Galli,[1] Koichi Kokame,[2] and Maurizio Molinari[1,3,*]
[1]Institute for Research in Biomedicine, Protein Folding and Quality Control, 6500 Bellinzona, Switzerland
[2]Department of Molecular Pathogenesis, National Cerebral and Cardiovascular Center, Osaka 565-8565, Japan
[3]Ecole Polytechnique Fédérale de Lausanne, School of Life Sciences, 1015 Lausanne, Switzerland
*Correspondence: maurizio.molinari@irb.usi.ch
http://dx.doi.org/10.1016/j.molcel.2013.10.016

SUMMARY

Folding-defective proteins must be cleared efficiently from the endoplasmic reticulum (ER) to prevent perturbation of the folding environment and to maintain cellular proteostasis. Misfolded proteins engage dislocation machineries (dislocons) built around E3 ubiquitin ligases that promote their transport across the ER membrane, their polyubiquitylation, and their proteasomal degradation. Here, we report on the intrinsic instability of the HRD1 dislocon and the constitutive, rapid turnover of the scaffold protein HERP. We show that HRD1 dislocon integrity relies on the presence of HRD1 clients that interrupt, in a dose-dependent manner, the UBC6e/RNF5/p97/proteasome-controlled relay that controls HERP turnover. We propose that ER-associated degradation (ERAD) deploys autoadaptive regulatory pathways, collectively defined as ERAD tuning, to rapidly adapt degradation activity to misfolded protein load and to preempt the unfolded protein response (UPR) activation.

INTRODUCTION

The endoplasmic reticulum (ER) is a site of synthesis and maturation of about 30% of the eukaryotic proteins. This membrane-bound organelle faces a continuous, physiologic production of byproducts of protein biogenesis, which results from the innate inefficiency of protein folding programs (Braakman and Hebert, 2013). The ER load with folding-defective polypeptides may fluctuate and depends on variations in the level of protein synthesis, inherited or sporadic mutations causing polypeptide misfolding, infections, perturbation of the folding environment, aging, and other factors. Misfolded proteins must rapidly be removed from the folding compartment as a prerequisite for maintenance of cellular proteostasis and survival (Balch et al., 2008; Brodsky, 2012; Lindquist and Kelly, 2011; Merulla et al., 2013; Walter and Ron, 2011). Aberrant gene products are delivered at the ER membrane to be retrotranslocated (dislocated) into the cytosol, polyubiquitylated, and degraded by 26S proteasomes in a series of events collectively defined as ER-associated degradation (ERAD; Brodsky, 2012). The activity of the ERAD machinery must be adjusted to the luminal load of misfolded polypeptides. Excessive ERAD may in fact interfere with completion of folding programs by inappropriately selecting not-yet-native folding intermediates for destruction, while insufficient ERAD leads to toxic accumulation of misfolded protein conformers (Bernasconi and Molinari, 2011). Recent evidences hint at direct roles of misfolded polypeptides in regulating ERAD activity by stabilizing otherwise rapidly turned over ERAD factors, by inhibiting the constitutive segregation of ERAD factors from the ER, or by promoting the assembly or inhibiting the disassembly of functional ERAD machineries in a series of posttranslational regulatory events, collectively defined as ERAD tuning (Merulla et al., 2013).

With a constitutive proteasome-regulated half-life of 1 hr, HERP is one example of rapidly turned over ERAD factor (Hori et al., 2004; Miura et al., 2010; Sai et al., 2003). The involvement of HERP in ERAD has been reported, as well as its participation in the evolutionarily conserved dislocation machinery built around the E3 ubiquitin ligase HRD1 that also comprises the adaptor protein SEL1L, the rhomboid pseudoprotease DER1, and a series of membrane-embedded, luminal, and cytosolic-associated factors (Bernasconi et al., 2010a; Christianson et al., 2012; Eura et al., 2012; Gao et al., 2010; Horn et al., 2009; Iida et al., 2011; Kim et al., 2008; Kny et al., 2011; Kokame et al., 2000; McLaughlin et al., 2010; Okuda-Shimizu and Hendershot, 2007; Sato et al., 2012; Schulze et al., 2005; Stolz et al., 2010; van Laar et al., 2000). However, the function of HERP in the HRD1 dislocation machinery is not understood.

Experiments in *S. cerevisiae*, where mammalian HERP complements, at least partially, some of the functions of Usa1p in the null mutant, imply that HERP might be the functional equivalent of yeast Usa1p (Carvalho et al., 2006). Usa1p acts as a scaffold that promotes assembly, maintains the integrity, and activates the ubiquitylation activity of the Hrd1p dislocon (Carroll and Hampton, 2010; Carvalho et al., 2006; 2010; Horn et al., 2009; Kanehara et al., 2010; Kim et al., 2009).

The short half-life distinguishes HERP from most ER-resident proteins, whose turnover is slow (Cambridge et al., 2011; Price et al., 2010). The peculiar instability of HERP compared to the stability of the other components of the HRD1 dislocation machinery, which are characterized by half-lives exceeding 30 hr, also violates the rule asserting that turnover rates of constituent subunits of multimeric complexes often fall within a small range (Cambridge et al., 2011; Price et al., 2010). Altogether, these observations led us to hypothesize that regulated HERP

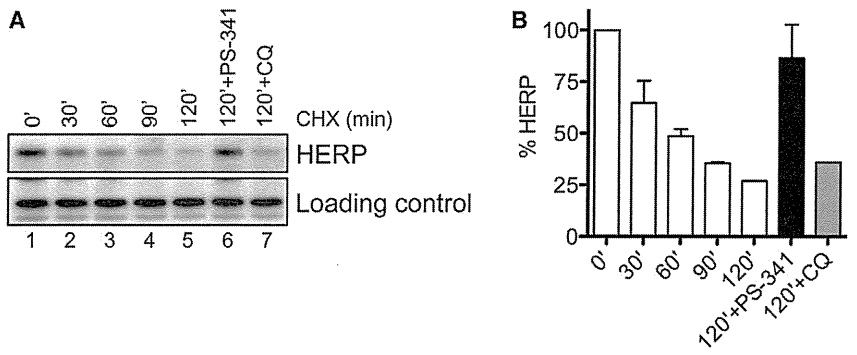

Figure 1. HERP Is a Short-Living ERAD Factor

(A and B) Turnover of endogenous HERP in HEK293 cells was analyzed by CHX chase followed by western blot (A) and quantified (B). The loading control is actin. PS-314 and chloroquine (CQ) are proteasomal and lysosomal inhibitors, respectively. Error bars: SD from the mean of three replicates.

turnover could set the activity of the ERAD machinery by determining the integrity of HRD1 dislocons.

Our analysis of endogenous HRD1 dislocons in cells expressing tunable levels of folding-defective HRD1 clients revealed an unexpected dynamicity of these supramolecular complexes. We report that HRD1 dislocons and the scaffold protein HERP are unstable when not engaged by clients. The constitutively rapid turnover of endogenous HERP is regulated by the E2 ubiquitin-conjugating enzyme UBC6e, the E3 ubiquitin ligase RNF5, the p97/UFD1 complex, and the 26S proteasome. Expression of HRD1 clients stabilizes HRD1 dislocons and delays, in a dose-dependent manner, turnover of endogenous HERP by inhibiting its RNF5-dependent recognition and polyubiquitylation. These findings highlight a mechanism of autoadaptive ERAD, where the integrity of dislocation machineries directly depends on the ER load with folding-defective clients.

RESULTS

The Constitutive HERP Turnover Is Regulated by UBC6e, RNF5, UFD1, p97, and the 26S Proteasome

Unlike other components of the HRD1 dislocon, such as HRD1, SEL1L, DER1, AUP1, UBXD2, BAP31, ERLIN1, ERLIN2, and others (Cambridge et al., 2011; Christianson et al., 2012), endogenous HERP has a much shorter half-life regulated by the ubiquitin proteasome system (UPS) ($t_{1/2}$ of about 60 min; Figures 1A, lanes 1–5, and 1B) (Hori et al., 2004; Miura et al., 2010; Sai et al., 2003). Consistently, HERP turnover was substantially inhibited upon inactivation of 26S proteasomes with PS-341 and remained unaffected upon cell exposure to lysosomotropic agents such as chloroquine (Figures 1A, lanes 6 and 7, respectively, and 1B).

To identify the components of the UPS involved in HERP turnover, we first monitored variations in the intracellular level and in the half-life of endogenous HERP upon silencing of select ER membrane-embedded E3 ubiquitin ligases. Individual silencing of HRD1, gp78, RNF103, or RNF166 or combined silencing of HRD1 and gp78 (Figures 2A, S1A, and S1B available online) did not significantly alter the intracellular level (Figures 2A, lanes 1–4, 6, and 7, and 2B) or the turnover (not shown) of endogenous HERP. In contrast, silencing of RNF5 delayed HERP turnover (Figures 2C, lanes 4–6 versus 1–3, and 2D), thus resulting in a 3-fold raise of the intracellular levels of HERP (Figures 2A, lane 5, 2B, 2C, lane 4 versus 1, 2E, lanes 2–4, and 2F). The intraluminal level of other ER-resident proteins (e.g., CNX, ERp72, BiP, and GRP94 in Figures 2A, 2C, and 2E) remained unchanged upon RNF5 silencing.

To identify the E2 ubiquitin-conjugating enzyme participating in the constitutive, RNF5-regulated turnover of HERP, we silenced the expression of UBC7, which has a reported role in ERAD (Webster et al., 2003), and UBC6e, the RNF5-associated E2 enzyme (Younger et al., 2006). As a positive control, the silencing of RNF5 with three different siRNAs substantially increased the intracellular level of endogenous HERP (Figures 2E, lanes 2–4, and 2F). While the downregulation of UBC7 had no effect (Figures 2E, lane 5, 2F, and S1C), the silencing of UBC6e with two different siRNAs substantially raised the level of HERP (Figures 2E, lanes 6 and 7, and 2F). Likewise, HERP levels substantially increased upon silencing of UFD1, which selectively recruits polyubiquitylated polypeptides to the p97 segregase (Ye et al., 2001) (Figures 2E, lane 9, 2F, and S1D–S1F), or upon cell incubation with N^2,N^4-dibenzylquinazoline-2,4-diamine (DBeQ), which selectively inactivates p97 (Figures S1E and S1F) (Chou et al., 2011).

Consistent with the involvement of the UPS in the turnover of endogenous HERP, cell exposure to the proteasomal inhibitor PS-341 caused the accumulation of polyubiquitylated HERP (Figure 2G, lane 2 versus 1, refer to Experimental Procedures) (Sai et al., 2003). Silencing of RNF5 (Figure 2G, lane 3) or UBC6e (lane 4) reduced the amount of polyubiquitylated HERP upon proteasomal inactivation, thus confirming RNF5 and UBC6e intervention in the rapid constitutive clearance of endogenous HERP from the mammalian ER.

As an additional indication of the role of RNF5 in the regulation of constitutive HERP turnover, coprecipitation analysis revealed a direct association between RNF5 and HERP at steady state (Figures 2H, first panel, lane 1, and S2A). Significantly, expression of the folding-defective protein Null Hong Kong (NHK), a client of the HRD1 dislocation machinery engaging HERP for efficient clearance from the ER (Figures S3 and S4A) (Kny et al., 2011), dose-dependently inhibited the RNF5:HERP interaction that regulates HERP turnover (Figure 2H, first panel) and dose-dependently favored HERP:HRD1 (second panel), HERP:SEL1L (fourth panel), and HRD1:SEL1L (fifth panel) interactions as an indication that engagement by clients stabilizes HRD1 dislocons, thereby protecting HERP from RNF5-controlled turnover.

Selective, Transcription-Independent Raise in Endogenous HERP Protein Levels in Cells Expressing a Folding-Defective HRD1 Client

Expression of a client of the HRD1 dislocation machinery, the folding-defective protein NHK, inhibits HERP recognition by

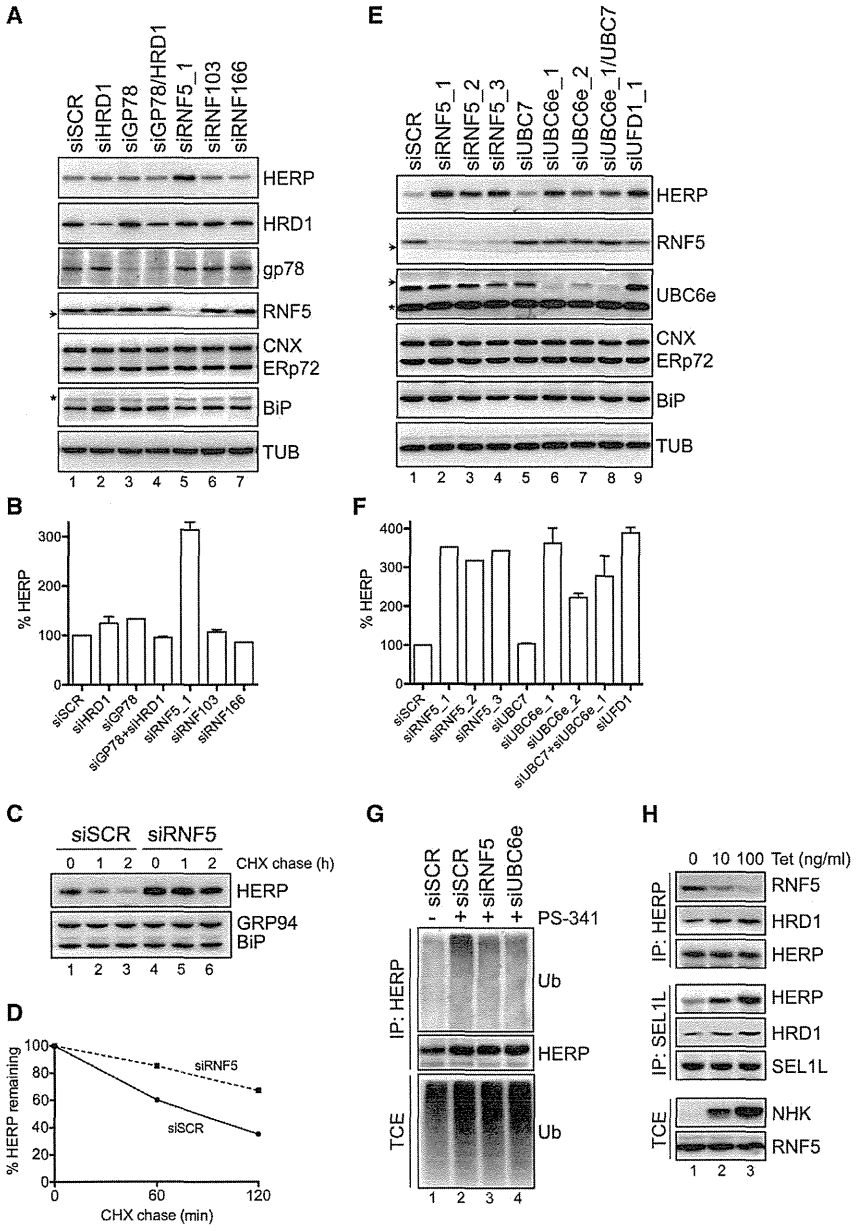

Figure 2. The E3 Ligase RNF5, the E2 Conjugating Enzyme UBC6e, and UFD1 Regulate the Constitutive Turnover of Endogenous HERP

(A) Levels of HERP, HRD1, gp78, RNF5, CNX, ERp72, BiP, and tubulin (TUB) (western blots) in mock cells (siSCR) or upon silencing of select genes. The arrow shows the end of the membrane. The asterisk shows a cross-reacting protein.

(B) Variations in the level of HERP were quantified and plotted.

(C and D) HERP turnover, BiP, and GRP94 levels were analyzed by CHX chase in mock cells (siSCR, lanes 1–3) and in RNF5-silenced cells (siRNF5, lanes 4-6) (C) and quantified (D).

(E) Levels of HERP, RNF5, UBC6e, CNX, ERp72, BiP, and tubulin (TUB) (western blots) in mock cells (siSCR) or upon silencing of select genes. The arrows show the end of the membrane (RNF5) or a cut in the membrane (UBC6e). The asterisk shows a cross-reacting protein.

(F) Same as in (B).

(G) Polyubiquitylation of HERP immunoisolated from mock (siSCR), RNF5-, or UBC6e-silenced cells incubated for 2 hr in the presence of PS-341 (+). Total cell extract (TCE) shows the total level of polyubiquitylated proteins.

(H) HERP:RNF5, HERP:HRD1, HERP:SEL1L, and HRD1:SEL1L complexes were monitored in cells expressing increasing amount of NHK (induction with 10–100 ng/ml tetracycline for 5 hr). Endogenous HERP (panels 1–3) or SEL1L (panels 4–6) was immunoisolated from lysates, and the associated *endogenous* RNF5, HRD1, or HERP was revealed by western blot. Please note that the samples for the anti-HERP immunoprecipitations have been normalized (third panel). TCE, total cell extract. Error bars: SD from the mean of three replicates.

RNF5, the E3 ubiquitin ligase that regulates the rapid, constitutive HERP turnover (Figure 2). We hypothesized that as a direct consequence, NHK expression might stabilize endogenous HERP engaged in the HRD1 dislocon. This could have important consequences on the activity of the HRD1 pathway since, at least in yeast, it has been shown that the HERP ortholog Usa1p regulates the integrity and the activity of the HRD1 dislocation machinery controlling misfolded protein clearance from the ER lumen (Carroll and Hampton, 2010; Carvalho et al., 2006; 2010; Horn et al., 2009; Kanehara et al., 2010; Kim et al., 2009).

NHK is a soluble, folding-defective polypeptide. It is classified as an ERAD-L_S substrate (Figure S3), and its clearance from the ER stringently relies on engagement of the HRD1 pathway (Bernasconi et al., 2010a). ERAD-L_S substrates are delivered to the ER membrane by the ERAD lectins OS-9 and XTP3-B (Bernasconi et al., 2008; Christianson et al., 2008; Hosokawa et al., 2008) and are retrotranslocated into the cytosol for proteasomal degradation by the HRD1 dislocon comprising HERP, the adaptor SEL1L, and the rhomboid pseudoprotease DER1 (Bernasconi et al., 2010a; Christianson et al., 2008; Greenblatt et al., 2011; Kny et al., 2011). All in all, NHK is a bona fide client of the HRD1 pathway that relies on HERP for efficient disposal from the ER (Figures S4A, lanes 1–6, and S4B) (Kny et al., 2011).

The analysis of a human embryonic kidney 293 (HEK293) cell line characterized by tetracycline-inducible expression of NHK (Figure 3A, first panel) revealed early responses to expression of the folding-defective transgene consisting of the selective raise of endogenous HERP levels (Figures 3A, second panel, and 3B, white columns). The induction of NHK expression did not affect the protein level of the two conventional ER stress markers BiP and GRP94 or of other components of the HRD1

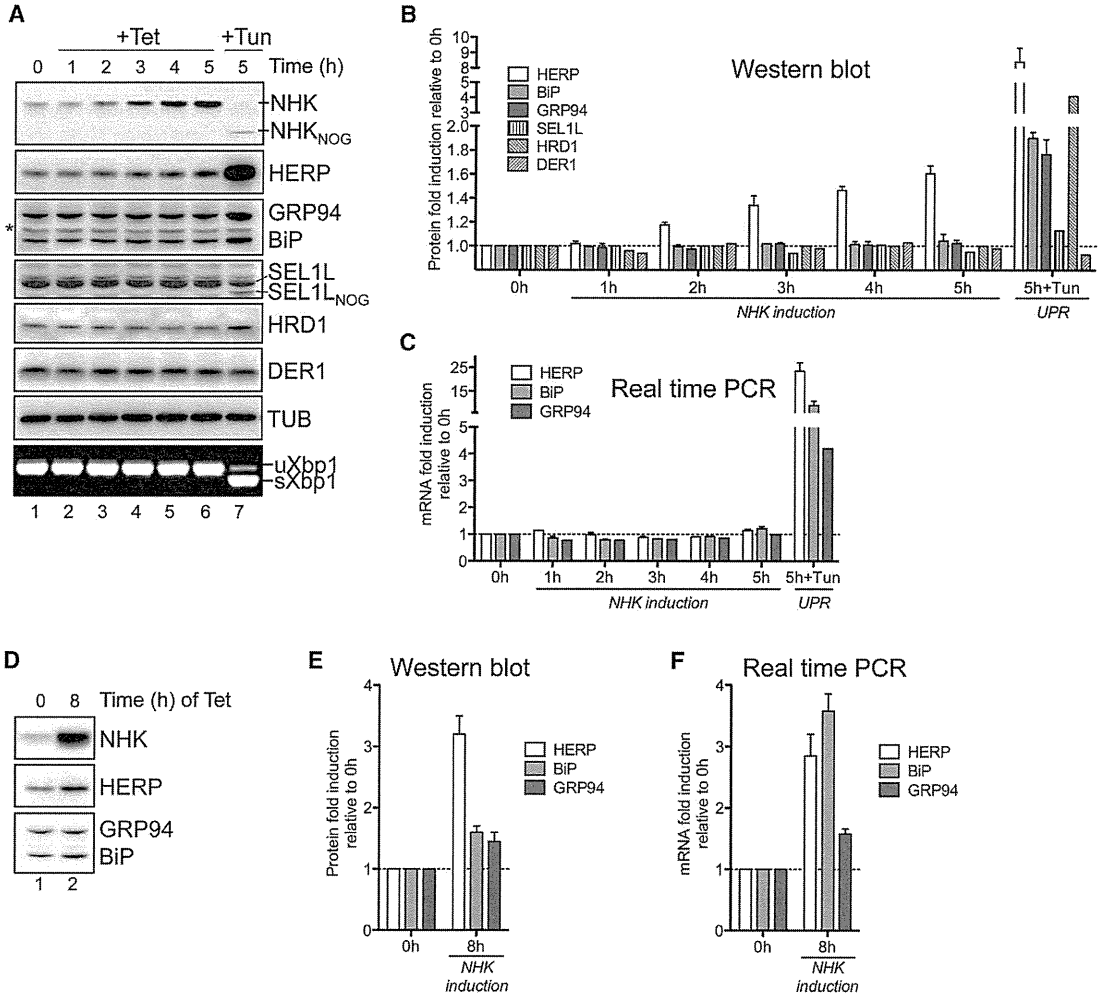

Figure 3. Short-Term Expression of Misfolded Proteins Induces a Specific UPR-Independent Accumulation of HERP

(A) Levels of NHK, HERP, GRP94, BiP, SEL1L, HRD1, DER1, and tubulin (TUB) (western blots) and of the transcript for spliced (s) and unspliced (u) Xbp1 (RT-PCR, last panel) after 0–5 hr NHK induction with 100 ng/ml tetracycline. In lane 7, UPR was induced with 5 hr exposure to 2.5 μg/μl tunicamycin (Tun). Please note the appearance of deglycosylated (NOG) NHK and SEL1L upon addition of Tun. The asterisk shows a cross-reacting protein.

(B) Quantification of HERP, BiP, GRP94, SEL1L, HRD1, and DER1 protein levels.

(C) Same as (B) for transcripts (quantitative RT-PCR).

(D) Levels of NHK, HERP, GRP94, and BiP (western blot) after 8 hr NHK induction with 100 ng/ml tetracycline.

(E) Same as in (B).

(F) Same as in (C).

Error bars: SD from the mean of two replicates.

dislocon (i.e., SEL1L, HRD1, DER1; Figures 3A and 3B). Quantitative RT-PCR revealed that the accumulation of the HERP protein upon NHK induction could not be ascribed to the activation of transcriptional UPR programs. In fact, the levels of HERP, BiP, and GRP94 transcripts did not increase (Figure 3C), and variations in Xbp1 splicing were not observed (Figure 3A). This early response to expression of NHK consisting of the elevation of HERP protein levels in the absence of transcriptional induction anticipated the induction of the UPR. In fact, induction of HERP, BiP, and GRP94 transcription did occur upon prolonged expression of higher concentrations of NHK (Figures 3D–3F) or when cells were subjected to widespread stress stimuli such as exposure to tunicamycin for 5 hr (Figures 3A, lane 7, 3B, and 3C).

HRD1 Client-Induced Delay of HERP Turnover

Since NHK inhibits, in a dose-dependent manner, the recognition of HERP by the E3 ubiquitin ligase RNF5, which controls polyubiquitylation and constitutive turnover of HERP (Figure 2H), we predicted that the transcription-independent raise of HERP protein in cells expressing NHK resulted from a client-induced delay of the constitutively rapid HERP turnover. To verify this, the half-life of endogenous HERP was monitored by cycloheximide (CHX) chase in cells incubated for 5 hr in the absence